Chapter 8

Estimation and Control in Time-delayed Dynamical Systems Using the Chebyshev Spectral Continuous Time Approximation and Reduced Liapunov-Floquet Transformation

Eric A. Butcher, Oleg Bobrenkov, Morad Nazari, Shahab Torkamani

New Mexico State University, Las Cruces, NM, 88003*, USA*
eab@nmsu.edu

In this chapter, a detailed description is provided of the authors' recent work on estimation and control of retarded time-delayed systems with (possibly) time-periodic coefficients using the Chebyshev spectral continuous time approximation (CSCTA) and reduced Liapunov-Floquet transformation (RLFT). First, these specialized computational tools are outlined and illustrated with several examples including various forms of the delayed Mathieu equation with single and multiple discrete delays as well as discontinuous distributed delay. Specifically, it is demonstrated how a time-periodic linear delayed system may be transformed into a set of constant-coefficient ODEs of low dimension in which the eigenstructure (including the dominant characteristic exponents of the delayed system) is exactly preserved in the transformed domain. Next, the control problem of (possibly time-periodic) time-delayed systems is explored, in which three strategies are suggested for designing closed-loop linear feedback controllers. Specifically, it is shown that using CSCTA and RLFT enables the control design to take place in the transformed coordinate system in which both the delay and periodic coefficients are effectively removed, thereby enabling the use of traditional control design tools for linear time-invariant systems. Next, the problem of estimation of states and parameters (including the delay) for nonlinear delayed systems using optimal stochastic filtering with noise-corrupted, possibly incomplete measurements is explored using CSCTA. After discretizing the delayed system with a set of ordinary differential equations, the stochastic estimation problem is implemented via the use of state augmentation and an extended Kalman-Bucy filter. This estimator can also be employed in an observer-based feedback controller, and for an illustrative example in a practical engineering problem, the problem of spacecraft attitude estimation and multi-actuator regulation control in the presence of time delay in one actuator is discussed and illustrated.

1. Introduction

Time-delayed dynamical systems, due to the vast variety of fields in science and engineering they can be relevant to, have attracted an increasing interest during past few decades. Papers on the stability analysis of delay differential equations (DDEs) started to appear in the 1940s. Unlike in the case of ODEs, dependence of the

current state derivative on the past state at prior times brings additional complexity to the stability analysis of DDEs. One of the first approaches was Krasovskii's generalization of the second method of Liapunov[1]. Various other methods were developed and various problems associated with the stability analysis of DDEs were posed. Some fundamental results in the frequency domain were obtained by Pontryagin[2], while Chebotarev and Meiman[3] and Hayes[4] studied the Routh-Hurwitz problems of quasi polynomials. Similar to the stability of linear time-invariant (LTI) ODEs which are usually analyzed through the computation of characteristic values of the state matrix, or equivalently the computation of the roots of the characteristic equation, for LTI DDEs this characteristic equation is represented by an exponential polynomial with an infinite number of complex roots. Different frequency domain stability criteria which take into account robustness and computational considerations appeared in 1990's and were closely connected to the rapid development of computer technologies. The theory of analysis and control of DDEs is covered in several modern texts, e.g., Refs.5–10.

Most stability and control studies of time-delayed systems assume single or multiple discrete delays. However, whenever the past effect of the system is distributed over an interval, distributed delay terms appear in the system model. Analysis of a system modeled by a DDE having distributed delay, or as it is called in some references a "Delayed Integro-Differential Equation" (DIDE), is more complicated than that for a system with discrete delays, e.g., Ref.11, and can include the case in which the distributed delay is discontinuous[12]. Distributed delay has been used to model the chip formation process in milling dynamics[13] and also can be used in delayed feedback control[14].

Two of the first studies on time-periodic systems with time delay were due to Hahn[15] and Stokes[16]. Recently, much attention has been devoted to the topic, e.g., Refs.7, 17 and references therein. Most of this work has been concerned with the stability problem in machining dynamics, in particular the problem of chatter vibrations in milling, e.g., Ref.18. In such problems, frequently the time-periodic coefficients of the DDE are discontinuous[19], which is a fundamentally different problem than that when the distributed delay is discontinuous in a DIDE. When either ODEs or DDEs have time-periodic coefficients, finding solutions analytically is rarely possible. Stability analysis for periodic ODEs requires computing the characteristic values (Floquet multipliers) of the finite-dimensional monodromy matrix[20], which is obtained by evaluating the state transition matrix at the principal parametric period. For periodic DDEs, however, the Floquet multipliers are eigenvalues of an infinite-dimensional monodromy operator. The positions of the dominant Floquet multipliers with respect to the unit circle in the complex plane should be analyzed. According to the unit circle stability criteria, if all eigenvalues lie within the unit circle then the system is asymptotically stable.

There have been a few research studies concerning state estimation and parameter identification for time delay systems, e.g., Refs.21–30. While in most of

these studies the critical role of measurement noise and model uncertainties is ignored, in Refs.22, 23 the optimal joint filtering and identification of states and parameters in a linear stochastic time delay system is studied through designing an optimal finite-dimensional filter. Parameter identification or state estimation of time-varying DDEs, however, has been treated in Refs.29, 30. There has also been much research in the literature concerning controller design for time-delayed systems, e.g., Refs.8, 9, 14, 31–41, including the case of delayed feedback control in which there is no choice but to use delayed states for feedback because the current states are simply not available. Unlike the case with the estimation problem, however, the control of periodic delayed systems has lately received significant attention, e.g., Refs.7, 17, 42–51.

Recently, new computational tools have been demonstrated that enable many of the traditional tools for time-invariant non-delayed systems to be successfully applied to various kinds of DDEs, including DIDEs and DDEs with periodic coefficients. These include the Chebyshev Spectral Continuous Time Approximation (CSCTA)[52], and the Reduced Liapunov-Floquet Transformation (RLFT)[53]. These specialized computational tools can be used in conjunction with estimation and control problems in time-delayed systems. This work explores the application of CSCTA and RLFT to the problems of estimation of parameters, states, and time delay as well as delayed feedback control of nonlinear delay differential equations (DDEs) having time-varying coefficients and discrete or distributed delay. In particular, a novel approach in state, parameter, and delay estimation of DDEs is proposed through exploiting optimal stochastic filtering in conjunction with CSCTA. The nonlinear delay differential equation is first discretized with a set of ordinary differential equations for which the stochastic estimation problem of the resulting ODE system is represented as an optimal filtering problem using a state augmentation technique. The extended Kalman-Bucy filter is used to obtain the estimated states, parameters, and delay from a noise-corrupted, possibly incomplete measurement of the states.

In addition, the control problem of time-delayed systems is also explored, in which both CSCTA and RLFT can be used for strategic advantage in designing delayed feedback controllers. For linear periodic time-delayed systems, this enables the control design to take place in a reduced order transformed coordinate system in which both the delay and periodic coefficients are effectively removed, thereby enabling the use of traditional tools for non-delayed LTI systems, while for nonlinear systems the linear part is transformed thus enabling the use of many additional tools for analysis and control of nonlinear systems. The estimator described above can also be employed to provide estimated states to be used in the feedback controller using an observer-based controller.

For an illustrative example of the above concepts in a practical engineering problem, the problem of attitude estimation and multi-actuator regulation control of a rigid spacecraft in the presence of time delays in one actuator is discussed.

A nonlinear feedback controller is designed using both delayed and non-delayed states such that the controlled system has the desired linear closed-loop dynamics which contains a time-delayed term using an inverse dynamics approach. First, the closed-loop stability is shown to be approximated by a second order linear DDE for the attitude coordinate for which the Hsu-Bhatt-Vyshnegradskii stability chart can be used to choose the control gains that result in a stable closed-loop response. It is shown that the suggested control methodology which was recently proposed in Ref.40 is an effective strategy for the problem of spacecraft attitude control using delayed feedback. Finally, the optimal estimator is combined with the controller in order to implement observer-based delayed feedback control of the spacecraft attitude with unknown time delay using optimally estimated states and delay obtained from noise-corrupted measurements.

2. Chebyshev Spectral Continuous Time Approximation

2.1. *Formulation*

In Refs.54–56, it was demonstrated that for a LTI DDE, an equivalent abstract LTI ODE can be introduced in which the infinite-dimensional system matrix is the infinitesimal generator of the solution operator. Previously, other strategies discretized the infinitesimal generator for constant DDEs via approximation of the derivatives using a finite difference-based differentiation[37,57] and pseudospectral differencing[58–60]. While it is predictable that the (linear) convergence of finite difference-based differentiation is slower than the (exponential) convergence of pseudospectral differencing[61], the efficiencies of both approaches were directly compared in the context of the stability analysis of specific DDEs in Ref.52. In addition, by approximating the equivalent abstract ODE a large set of tools for analysis, estimation, and control of ODEs becomes available to use with DDEs. It is noted that other techniques such as the Galerkin method (e.g., Ref.62) have also been presented to obtain a set of ODEs from DDEs.

In this section, a new CSCTA technique which was recently introduced in Ref.52 will be reviewed. This technique allows for a DDE system to be represented as a larger system of ODEs. The advantages of this technique are that the nonlinearities and external excitation can be simply incorporated in the formulation. Also, this technique is applicable to constant and periodic DDEs with multiple delays, as well as DIDEs with discontinuous distributed delay.

Consider a system of nonlinear retarded autonomous DDEs with a single discrete time delay described by

$$\begin{aligned} \dot{\mathbf{x}}(t) &= \mathbf{A}_1\mathbf{x}(t) + \mathbf{A}_2\mathbf{x}(t-\tau) + \mathbf{f}(\mathbf{x}(t), \mathbf{x}(t-\tau)), \\ \mathbf{x}(t) &= \phi(\theta), \quad -\tau \le t = \theta \le 0, \end{aligned} \tag{1}$$

where $\mathbf{x} \in \mathbb{R}^q$ is a q-dimensional state vector, $\mathbf{A}_1$ and $\mathbf{A}_2$ are constant $q \times q$ matrices, $\mathbf{f}(\cdot)$ is a nonlinear q-dimensional vector function of the current and delayed states,

and $\phi(t)$ is the initial vector function. As explained in Refs.54–56, the abstract representation of Eq.(1) is the evolution of an initial function in a Banach space, i.e.,

$$\dot{\mathcal{Y}}(t) = \mathcal{A}\mathcal{Y}(t) + \mathcal{F}(\mathcal{Y}(t)), \quad \mathcal{Y}(0) = \phi(\theta) \tag{2}$$

where $\mathcal{Y}(t)$ and $\mathcal{F}(\cdot)$ are infinite-dimensional vectors and $\mathcal{A}$ is the infinitesimal generator of the solution operator corresponding to the linearized system, i.e.,

$$\mathcal{T}(t) : \mathcal{C}\left([-\tau, 0], \mathbb{R}^q\right) \rightarrow \mathcal{C}\left([-\tau, 0], \mathbb{R}^q\right) = \frac{\partial \mathcal{Y}(t)}{\partial \phi} \tag{3}$$

that maps the initial function deviations $\delta\phi$ forward in time. This operator is a strongly continuous semigroup, and it satisfies all the semigroup properties including $\mathcal{T}(0) = I$, $\mathcal{T}(t)\mathcal{T}(s) = \mathcal{T}(t+s)$. The infinitesimal generator $\mathcal{A}$ is defined as

$$\begin{aligned}
&\mathcal{A}\phi = \frac{d\phi}{d\theta} = \lim_{t\to 0} \frac{1}{t}\left(\mathcal{T}(t)\phi - \phi\right), \ -\tau \le \theta < 0, \\
&\mathcal{A}\phi = \mathbf{A}_1\mathbf{x}(0) + \mathbf{A}_2\mathbf{x}(-\tau), \quad \theta = 0, \\
&\mathcal{A}\phi + \mathcal{F}(\phi) = \mathbf{A}_1\mathbf{x}(0) + \mathbf{A}_2\mathbf{x}(-\tau) + \mathbf{f}(\mathbf{x}(0), \mathbf{x}(-\tau)), \quad \theta = 0
\end{aligned} \tag{4}$$

and can be thought of as an infinite-dimensional square matrix. Approximation of the infinite dimensional vectors $\mathcal{Y}(t)$ and $\mathcal{F}(\cdot)$ and operator $\mathcal{A}$ with finite dimensional ones is the main idea of CSCTA.

Accordingly, the main steps are setting up an uneven grid of Chebyshev collocation points, fitting an interpolating polynomial through the values of the function evaluated at the grid points, and then differentiating the polynomial and evaluating the result at each grid point as a linear combination of the nodal function values[63]. The Chebyshev collocation points are unevenly spaced points in the domain $[-1, 1]$ corresponding to the extremum points of the Chebyshev polynomial of the first kind[64] of degree N. As seen in Fig. 1(a), we can also define these points as the projections of equispaced points on the upper half of the unit circle as $t_j = \cos(j\pi/N)$, $j = 0, 1, \ldots, N$ where the number of collocation points used is $m = N + 1$. The main advantage of this strategy lies in its "spectrally accurate" exponential convergence characteristics, which are significantly more desirable than those of finite difference, finite elements, cubic splines, or wavelets on analytic functions. In addition, the unequally spaced Chebyshev grid are nearly optimal interpolation points for minimizing uniform error compared with the zeros or extremum points of other orthogonal polynomials and avoid the Gibbs phenomenon of interpolating functions which are typically associated with an equally spaced grid.

Associated with the Chebyshev grid, we can find the $m \times m$ Chebyshev differ-

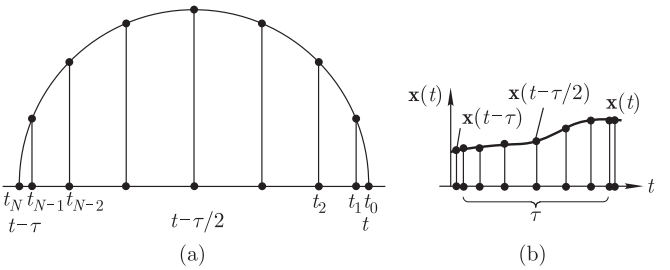

Fig. 1. Diagrams of (a) Chebyshev collocation points as defined by projections from the unit circle and (b) solution of $\mathbf{x}(t)$ discretized by CSCTA.

entiation matrix $\mathbf{D}_N$ for any order N using indices from 0 to N as Ref.61

$$\begin{aligned} D_{00} &= \frac{2N^2+1}{6}, \quad D_{NN} = -\frac{2N^2+1}{6}, \\ D_{jj} &= \frac{-t_j}{2(1-t_j^2)}, \quad j = 1, \ldots, N-1, \\ D_{ij} &= \frac{c_i(-1)^{i+j}}{c_j(t_i-t_j)}, \quad i \neq j,\ i,j = 0, \ldots, N, \\ c_i &= \begin{cases} 2, & i = 0, N, \\ 1, & \text{otherwise.} \end{cases} \end{aligned} \tag{5}$$

Also, let the $mq \times mq$ differential operator $\mathbb{D}$ (corresponding to q first order DDEs) be defined as $\mathbb{D}_{\mathbf{N}} = \mathbf{D}_{\mathbf{N}} \otimes I_q$, where I_q is a $q \times q$ identity matrix.

A finite dimensional approximation to $\mathcal{Y}(t)$ is now defined as

$$\begin{aligned} \mathbf{y}(t) &= \left[\, \mathbf{x}^T(t), \ldots, \mathbf{x}^T(t-\tau) \,\right]^T \\ &= \left[\, \mathbf{x}^T(t_0), \mathbf{x}^T(t_1), \mathbf{x}^T(t_2), \ldots, \mathbf{x}^T(t_N) \,\right]^T \\ &= \left[\, \mathbf{y}_1^T(t), \mathbf{y}_2^T(t), \mathbf{y}_3^T(t), \ldots, \mathbf{y}_m^T(t) \,\right]^T \end{aligned} \tag{6}$$

where $\mathbf{x}(t_0) = \mathbf{x}(t)$ and $\mathbf{x}(t_N) = \mathbf{x}(t-\tau)$ (see Fig. 1(b)). Equation (2) is now approximated as

$$\dot{\mathbf{y}}(t) = \hat{\mathbf{A}}\mathbf{y}(t) + \hat{\mathbf{f}}(\mathbf{y}(t)) \tag{7}$$

where $\hat{\mathbf{A}}$ is obtained from $\mathbb{D}_{\mathbf{N}}$ by (1) replacing the first q rows by zeros and (2) replacing the $q \times q$ left upper corner by the $\mathbf{A}_1$ matrix and the $q \times q$ right upper corner by the $\mathbf{A}_2$ matrix. The nonlinear vector $\hat{\mathbf{f}}(\cdot)$ is nonzero only on the first q elements which take the form $\mathbf{f}(\mathbf{y}_1(t), \mathbf{y}_m(t))$. Thus, equation (7) is as follows:

$$\begin{bmatrix} \dot{\mathbf{y}}_1(t) \\ \dot{\mathbf{y}}_2(t) \\ \vdots \\ \dot{\mathbf{y}}_m(t) \end{bmatrix} = \begin{bmatrix} \mathbf{A}_1 & \mathbf{0}_q & \cdots & \mathbf{0}_q & \mathbf{A}_2 \\ & & \frac{2}{\tau}\left[\mathbb{D}_{\mathbf{N}}\ {}^{(q+1,mq)}\right] & & \end{bmatrix} \begin{bmatrix} \mathbf{y}_1(t) \\ \mathbf{y}_2(t) \\ \vdots \\ \mathbf{y}_m(t) \end{bmatrix} + \begin{bmatrix} \mathbf{f}(\mathbf{y}_1(t), \mathbf{y}_m(t)) \\ 0 \\ \vdots \\ 0 \end{bmatrix} \tag{8}$$

where the superscript $(q+1, mq)$ on $\mathbb{D}_{\mathbf{N}}$ refers to the fact that only rows of $\mathbb{D}_{\mathbf{N}}$ between $q+1$ and mq are written into the remaining $Nq \times mq$ part of matrix $\hat{\mathbf{A}}$. Note that the $2/\tau$ factor in front of the portion of $\mathbb{D}_{\mathbf{N}}$ above accounts for the fact of rescaling the standard collocation expansion interval $[-1, 1]$ to $[0, \tau]$.

In Ref.12 a new extended CSCTA-based technique was introduced for the response and stability analysis of DDEs with the simultaneous effects of the periodic time variation of coefficients and of discontinuous distributed delay. To illustrate the extended formulation, consider a q-dimensional linear system of periodic DDEs with discontinuous distributed delay as

$$\begin{aligned} \dot{\mathbf{x}}(t) &= \mathbf{A}(t)\mathbf{x}(t) + \sum_{i=1}^{k} \int_{-\tau_i}^{-\tau_{i-1}} \boldsymbol{\eta}_i(\theta, t)\mathbf{x}(t+\theta)d\theta, \\ \mathbf{x}(t) &= \boldsymbol{\phi}(t), \quad -\max(\tau_i) \le t \le 0 \end{aligned} \tag{9}$$

where $\mathbf{A}(t+T) = \mathbf{A}(t)$ is a time-periodic matrix. Each $\boldsymbol{\eta}_i(\theta, t) = \boldsymbol{\eta}_i(\theta, t+T)$ is a matrix of periodic continuous functions valid in some time delay interval $\theta \in [-\tau_i, -\tau_{i-1}]$, $i = 1, 2, \ldots, k$. Equivalently, this sum of integrals can be expressed as $\int_{-\max(\tau_i)}^{0} \boldsymbol{\eta}(\theta, t)\mathbf{x}(t+\theta)d\theta$, where $\boldsymbol{\eta}(\theta, t)$ is periodic in t with period T and discontinuous in θ. Distributed delays in Eq.(9) can become discrete in the case when a $\boldsymbol{\eta}_i(\theta, t)$ matrix includes a Dirac delta function. The functions $\boldsymbol{\eta}_i(\theta, t)$ may also vanish in various intervals if the state derivative does not depend on the states in that interval.

Let the extended state vector $\mathbf{y}(t)$ be introduced as

$$\mathbf{y}(t) = \left[\mathbf{x}^T(t),\ \cdots,\ \mathbf{x}^T(t-\tau_1),\ \cdots,\ \mathbf{x}^T(t-\tau_{k-1}),\ \cdots,\ \mathbf{x}^T(t-\tau_k)\right]^T \tag{10}$$

where k is the number of discontinuous distributed delay terms and k separate Chebyshev grids each with m points are defined in each of the intervals $[t-\tau_i, t-\tau_{i-1}]$ of length h_i, $i = 1, 2, \cdots, k$. Therefore, as shown in Ref.12, equation (9) can be discretized as

$$\dot{\mathbf{y}}(t) = \hat{\mathbf{A}}(t)\mathbf{y}(t), \tag{11}$$

where

$$\hat{\mathbf{A}}(t) = \begin{bmatrix} \mathbf{A}(t)\ \mathbf{0}_2\ \cdots\ \mathbf{0}_2\ \mathbf{B}_{21}(t)\ \cdots\ \mathbf{B}_{2,m_2}(t)\ \cdots\ \mathbf{B}_{k1}(t)\ \cdots\ \mathbf{B}_{k,m_k}(t) \\ \begin{bmatrix} \frac{2}{h_1}\mathbb{D}_{N_1}^{(q+1,m_1 q)} \end{bmatrix} \\ \begin{bmatrix} \frac{2}{h_2}\mathbb{D}_{N_2}^{(q+1,m_2 q)} \end{bmatrix} \\ \ddots \\ \begin{bmatrix} \frac{2}{h_k}\mathbb{D}_{N_k}^{(q+1,m_k q)} \end{bmatrix} \end{bmatrix}, \tag{12}$$

$\mathbf{B}_{ij}(t)$ $(i = 1, 2, \ldots, k,\ j = 1, 2, \ldots, m_i)$ represent the matrix functions $\boldsymbol{\eta}_i(\theta, t)$ evaluated at the Chebyshev points of each interval multiplied by weighting coefficients based on Clenshaw-Curtis quadrature[61,65] and rescaled by a factor $h_i/2$ which allows a definite integral to be computed as a linear combination of the integrand values at the Chebyshev collocation points within the interval of integration.

The blocks $\frac{2}{h_i}\mathbb{D}_{N_i}^{(q+1,m_i q)}$ $(i = 1, 2, \ldots, k)$ in Eq.(12) are differential operators $\mathbb{D}_{N_i} = \mathbf{D}_{N_i} \otimes I_q$ (rescaled to account for intervals $[-\tau_i, -\tau_{i-1}]$) with the first q rows omitted. The number of Chebyshev collocation points for the ith interval is $m_i = N_i + 1$. The overlapping occurrences of the contiguous $\mathbb{D}_{N_i}^{(q+1,m_i)}$ blocks are due to the common nodes of the adjacent collocation intervals. The T-periodic matrix $\hat{\mathbf{A}}(t)$ introduced in Eq.(12) is a square matrix of order $\left(q\sum_{i=1}^{k} m_i\right)$. However, as was noted in Ref.12 this matrix is not an approximation to the infinitesimal generator but is simply the discretized matrix that results from rewriting the DDE as a boundary value problem, a strategy which is also valid for any linear or nonlinear DDE.

2.2. *Examples*

2.2.1. *First Order Scalar Linear DDE*

Consider the following scalar linear DDE with constant coefficients

$$\dot{x}(t) = -ax(t) - bx(t-\tau). \tag{13}$$

Assuming the solution in the form $x(t) = e^{\lambda t}$ yields the characteristic equation

$$\lambda + a + be^{-\lambda\tau} = 0. \tag{14}$$

The stability boundaries for the scalar DDE can be obtained analytically[9] by assuming $\lambda = 0$ as

$$a + b = 0 \tag{15}$$

and also by assuming $\lambda = \mathrm{i}\omega$ and separating the real and imaginary parts to obtain the delay dependent boundary

$$\tau\sqrt{b^2 - a^2} = \arccos\left(-\frac{a}{b}\right). \tag{16}$$

The number of first order equations equals one in this case, so matrices $\mathbf{A}_1 = -a$ and $\mathbf{A}_2 = -b$ in Eq.(8) are constant scalar parameters. The matrix $\hat{\mathbf{A}}$ for this

example with $m = 5$ collocation points and $\tau = 1$ is given by

$$\hat{\mathbf{A}} = \begin{bmatrix} -a & 0 & 0 & 0 & -b \\ 3.4142 & -1.4142 & -2.8284 & 1.4142 & -0.5858 \\ -1 & 2.8284 & 0 & -2.8284 & 1 \\ 0.5858 & -1.4142 & 2.8284 & 1.4142 & -3.4142 \\ -1 & 2.3431 & -4 & 13.6569 & -11 \end{bmatrix}. \tag{17}$$

Stability of the equilibrium solution of Eq.(13) is determined by the eigenvalues of $\hat{\mathbf{A}}$ via the left half plane stability criterion, i.e., the spectral abscissa $\alpha(\hat{\mathbf{A}})$ must be less than zero for asymptotic stability. Four stability boundaries are shown in Fig.2. For comparison purposes, forward and centered finite difference methods with equally-spaced grid points are also used to generate approximations to the infinitesimal generator. The dots indicate the plot of the curves in Eqs.(15) and (16), the thin solid line represents the stability chart obtained by CSCTA, the thick dashed line is the stability boundary obtained using centered finite differences as described in Ref.57, and the dash-dotted line is used for the forward finite difference boundary. It can be seen that 5 collocation points give sufficient accuracy for both stability boundaries, whereas the matrices resulting from finite differences yield an inaccurate Hopf stability boundary. (Note $\hat{\mathbf{A}}$ is 5×5 in all three cases.)

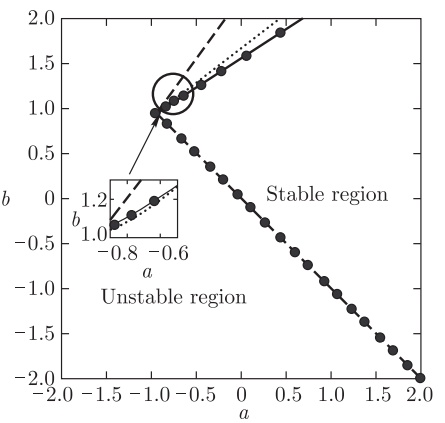

Fig. 2. Diagrams of stability of the scalar DDE (13) for $\tau = 1$ obtained analytically (dotted), by CSCTA (solid), CTA involving centered finite differences from Ref.57 (dashed), and forward finite differences (dash-dotted). Five collocation points and four finite differences were used to keep the same dimension of all approximate $\hat{\mathbf{A}}$ matrices.

Finally, in Fig. 3 the eigenvalues of the 20×20 and 40×40 $\hat{\mathbf{A}}$ matrices from the three approximation methods are compared with the exact roots of the characteristic equation. It is seen that CSCTA more accurately captures the true eigenvalue

spectrum compared with the method of finite differences which often produces spurious eigenvalues.

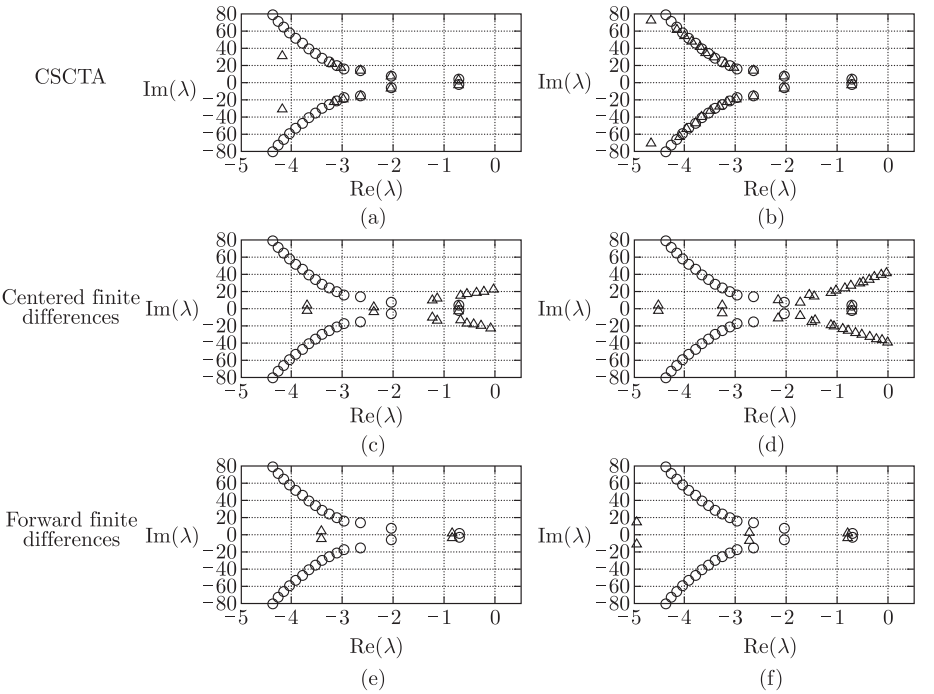

Fig. 3. Approximate eigenvalues (triangles) of the 20×20 (lst column) and 40×40 (2nd column) $\hat{\mathbf{A}}$ matrices resulting from CSCTA, centered finite differences, and forward finite differences compared with the exact roots of the characteristic equation (circles) for the scalar DDE in Eq.(13) for $\tau = 1$ and $(a, b) = (1.5, 1)$.

2.2.2. *Delayed Mathieu Equation with Discontinuous Distributed Delays*

Now consider the delayed Mathieu equation with discontinuous distributed delays given by

$$\ddot{x}(t) + (a + b\cos t)x(t) = c\,x(t - 2\pi) + \cos 2t \left(c_1 \int_{-0.6\pi}^{-0.2\pi} w_1(\theta)x(t + \theta)d\theta + c_2 \int_{-2\pi}^{-\pi} w_2(\theta)x(t + \theta)d\theta \right). \tag{18}$$

Note that the parametric period $T = \tau_{\max} = 2\pi$. To obtain the CSCTA form of Eq.(18) the submatrices in Eq. (12) are obtained as

$$\mathbf{A}(t) = \begin{bmatrix} 0 & 1 \\ -(a + b\cos t) & 0 \end{bmatrix},$$

$$\mathbf{B}_{ji}(t) = c_k W_{ji} \begin{bmatrix} 0 & 0 \\ w_k(\theta_{ji}) & 0 \end{bmatrix} \cos 2t, \quad k = 1, 2; \quad j = 2, 4,$$

$$i = \begin{cases} 1, 2, \cdots, m, & j = 2, \\ 1, 2, \cdots, m-1, & j = 4, \end{cases} \tag{19}$$

$$\mathbf{B}_{4,m}(t) = c_2 W_{4,m} \begin{bmatrix} 0 & 0 \\ w_2(\theta_{4,m}) & 0 \end{bmatrix} \cos 2t + \begin{bmatrix} 0 & 0 \\ c & 0 \end{bmatrix}$$

where $w_i(\theta_{ji})$ are Clenshaw-Curtis weights for the collocation points θ_{ji}. The monodromy matrices corresponding to Eq.(11) were subsequently obtained for various parameter sets and the stability determined from their eigenvalues (Floquet multipliers) by the unit circle criteria. Stability charts for Eq.(18) are shown in Fig. 4. The values of discontinuous distributed delay coefficients are changed simultaneously, and the stability charts in the (a, c) plane are shown. The first column of plots can be recognized as those of the standard delayed Mathieu equation (for $c_1 = c_2 = 0$)[66], which is turn are similar to both the Hsu-Bhatt-Vyshnegradskii stability chart for the constant second order time-delayed system[67] and the Strutt-Ince stability chart for the standard Mathieu equation[68].

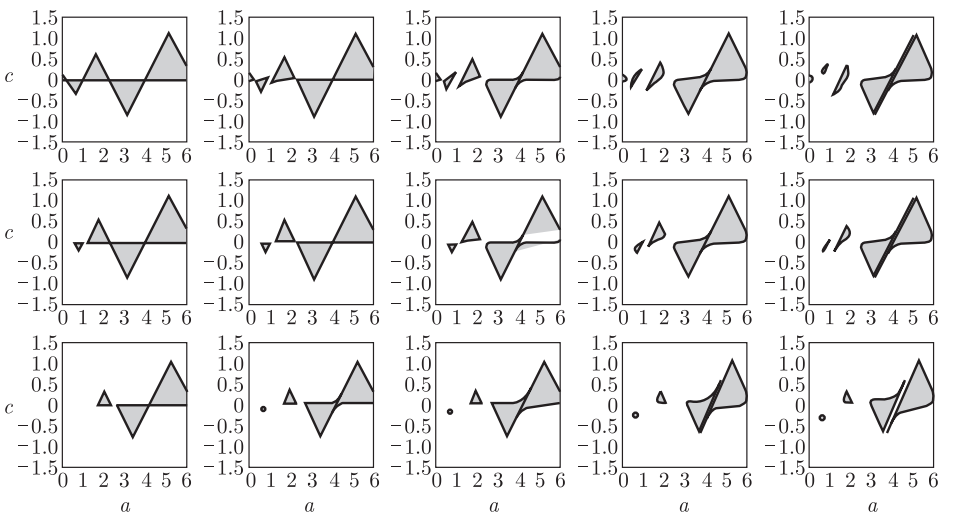

Fig. 4. Stability charts for Eq.(18) in the (a, c) plane for different values of b and $c_1 = c_2$. The parameter values are: $b = 0.1$, 1, and 2 in the first, second, and third row, respectively, and $c_1 = c_2 = 0$, 0.1, 0.2, 0.3, and 0.4 in the respective columns from 1 to 5. The shaded regions are stable.

3. Reduced Liapunov-Floquet Transformation

3.1. *Formulation*

As was discussed from a theoretical perspective in Ref.20 and from a practical perspective in Ref.69, application of the Liapunov-Floquet Transformation (LFT) enables the analysis of time-periodic ODEs by employing theoretical and computational tools for ODEs with time-invariant linear part. This approach was successfully implemented for various applications in linear and nonlinear time-periodic systems analysis such as order reduction[70,71], chaos and bifurcation control[72,73], construction of time-invariant forms[74], and Hamiltonian perturbations[75], among others.

In Ref.53, LFT was applied for the first time to a time-periodic linear DDE discretized by CSCTA. The proposed combined approach allows for the stability and time response analysis of the periodic DDE by applying a $2T$-periodic LFT to the equivalent large-order periodic ODE system resulting from CSCTA. It was shown, however, that the less accurate Floquet multipliers (which are clustered about the origin in the complex plane) do not allow the computation of the full-size LFT matrix. Therefore, a linear order reduction transformation must be applied which results in a RLFT and a corresponding reduced order constant ODE system which together contain the dominant modes and thus the approximate dynamics of the DDE. In fact, combining CSCTA and RLFT results in a new technique for the analysis of time-periodic nonlinear DDEs which is an alternative to the existing techniques for dimensional reduction such as center manifold analysis for nonlinear constant[76–78] and periodic nonlinear DDEs[79] and the multiple scales method[80] applied to nonlinear constant DDEs.

Consider the application of the standard LFT as[69]

$$\mathbf{y}(t) = \mathbf{L}(t)\mathbf{z}(t), \quad \mathbf{L}(t) = \mathbf{L}(t+T) \tag{20}$$

to Eq.(11) such that it is transformed to a time-invariant system as

$$\dot{\mathbf{z}}(t) = \mathbf{C}\mathbf{z}(t) \tag{21}$$

where $\mathbf{C}$ is a constant matrix, and $\mathbf{L}(t)$ is the T-periodic LFT matrix. Instead of the representation which uses the complex matrices $\mathbf{C}$ and $\mathbf{L}(t)$, equations (20) and (21) can be rewritten using the $2T$-periodic transformation with real matrices $\mathbf{R}$ and $\mathbf{Q}(t)$ as

$$\mathbf{y}(t) = \mathbf{Q}(t)\mathbf{z}(t), \quad \mathbf{Q}(t) = \mathbf{Q}(t+2T) \tag{22}$$

and

$$\dot{\mathbf{z}}(t) = \mathbf{R}\mathbf{z}(t). \tag{23}$$

It has been shown in Ref.69 that the LFT matrix $\mathbf{L}(t)$ can be computed in closed form for a commutative system for which the state transition matrix (STM) is known. If the system is not commutative, then the STM must be approximated,

for example by Chebyshev polynomial expansion[81]. In either case, the STM can be factored as

$$\mathbf{\Phi}(t) = \mathbf{L}(t)e^{\mathbf{C}t} = \mathbf{Q}(t)e^{\mathbf{R}t} \tag{24}$$

where

$$\mathbf{C} = \frac{1}{T}\ln\mathbf{\Phi}(T); \quad \mathbf{R} = \frac{1}{2T}\ln\mathbf{\Phi}(2T) \tag{25}$$

are computed via an eigenanalysis of the monodromy matrix $\mathbf{\Phi}(T)$ or its square $\mathbf{\Phi}(2T) = \mathbf{\Phi}^2(T)$. Therefore, the T- and $2T$-periodic matrices $\mathbf{L}(t)$ and $\mathbf{Q}(t)$ are solved as

$$\mathbf{L}(t) = \mathbf{\Phi}(t)e^{-\mathbf{C}t}, \quad \mathbf{Q}(t) = \mathbf{\Phi}(t)e^{-\mathbf{R}t} \tag{26}$$

and can be expressed as a real Fourier series up to some desired accuracy. Since we are interested in the real $2T$-periodic transformation, the future discussion will be around $\mathbf{Q}(t)$ rather than $\mathbf{L}(t)$.

As previously discussed, a RLFT is required in which only the r modes corresponding to r dominant Floquet multipliers are retained, since the inaccurate multipliers clustered around the origin result in a set of inaccurate eigenvalues of $\mathbf{R}$ (characteristic exponents) with highly negative real parts which in turn makes Eq.(26) impractical to compute the full LFT matrix. Often we choose $r = q$, that is, we retain the same number of modes as the size of the DDE. Therefore, consider an order reduction transformation $\mathbf{z} = \hat{\mathbf{T}}\mathbf{w}$ where

$$\hat{\mathbf{T}} = \mathbf{M}\mathbf{T}\mathbf{M}_{11}^{-1} = \begin{bmatrix} \mathbf{M}_{11} & \mathbf{M}_{12} \\ \mathbf{M}_{21} & \mathbf{M}_{22} \end{bmatrix} \begin{bmatrix} \mathbf{I}_q \\ \mathbf{0}_{(m-1)q\times q} \end{bmatrix} \mathbf{M}_{11}^{-1} = \begin{bmatrix} \mathbf{I}_q \\ \mathbf{M}_{21}\mathbf{M}_{11}^{-1} \end{bmatrix} \tag{27}$$

is a $mq \times q$ rectangular matrix. $\mathbf{M}$ is the modal matrix of $\mathbf{R}$ such that $\mathbf{R} = \mathbf{M}\mathbf{\Lambda}\mathbf{M}^{-1}$ and the matrix

$$\mathbf{\Lambda} = \begin{bmatrix} \mathbf{\Lambda}_1 & \mathbf{0} \\ \mathbf{0} & \mathbf{\Lambda}_2 \end{bmatrix} \tag{28}$$

is diagonal. Only the modal coordinates corresponding to $\mathbf{\Lambda}_1$ are retained. Also, $\mathbf{M}_{11}$ is the top left $q \times q$ partition of $\mathbf{M}$. Application to Eq.(23) yields

$$\dot{\mathbf{w}} = \bar{\mathbf{R}}\mathbf{w} \tag{29}$$

where $\bar{\mathbf{R}} = (\hat{\mathbf{T}}^T\hat{\mathbf{T}})^{-1}\hat{\mathbf{T}}^T\mathbf{R}\hat{\mathbf{T}}$ is a projection of matrix $\mathbf{R}$ onto $\mathbf{w}$ such that equation (29) exactly preserves the eigenstructure of Eq.(23). Note that in Eq.(27) $\mathbf{z}_1 = \mathbf{w}$ (master coordinates) and $\mathbf{z}_2 = \mathbf{M}_{21}\mathbf{M}_{11}^{-1}\mathbf{w}$ is the relation between master and slave coordinates where $\mathbf{z}^T = \begin{bmatrix}\mathbf{z}_1^T, & \mathbf{z}_2^T\end{bmatrix}$ is partitioned into vectors of length q and $(m-1)q$, respectively.

Because the state vector $\mathbf{x}(t)$ is actually a reduced subset of the first q elements of vector $\mathbf{y}(t)$, we define a RLFT matrix $\bar{\mathbf{Q}}(t)$ that transforms the original DDE in Eq.(11) into Eq.(29) and that satisfies

$$\mathbf{x}(t) = \mathbf{T}^T\mathbf{y}(t) = \mathbf{T}^T\mathbf{Q}(t)\mathbf{z}(t) = \bar{\mathbf{Q}}(t)\mathbf{w}(t) = \bar{\mathbf{Q}}(t)\mathbf{T}^T\mathbf{z}(t) \tag{30}$$

where $\mathbf{T}^T = [\mathbf{I}_q,\ \mathbf{0}_{q\times(m-1)q}]$. Hence,

$$\mathbf{T}^T\mathbf{Q}(t) = \bar{\mathbf{Q}}(t)\mathbf{T}^T \tag{31}$$

and the RLFT matrix may be obtained as

$$\bar{\mathbf{Q}}(t) = \mathbf{T}^T\mathbf{Q}(t)\mathbf{T} = \mathbf{Q}_{11}(t) \tag{32}$$

where $\mathbf{Q}_{11}(t)$ is the top left $q \times q$ partition of $\mathbf{Q}(t)$. Equation (32) represents a projection of the full LFT matrix. However, recall that it is impractical to compute $\mathbf{Q}(t)$ in its entirety to begin with. Therefore, we seek a simple way to obtain $\bar{\mathbf{Q}}(t)$ without computing $\mathbf{Q}(t)$. Recalling the form for $\mathbf{Q}(t)$ in Eq.(26), an analogous formula for an approximate $\bar{\mathbf{Q}}(t)$ that was used successfully in Ref.53 is

$$\bar{\mathbf{Q}}(t) = \mathbf{\Phi}_{11}(t)e^{-\mathbf{R}_{11}t} \tag{33}$$

where $\mathbf{\Phi}_{11}$ and $\mathbf{R}_{11}$ are the upper $q\times q$ partitions of $\mathbf{\Phi}(t)$ and $\mathbf{R}$, respectively. Note that the necessary initial condition at $t = 0$ for Eq.(32) is satisfied.

The transformations in Eqs.(20), (22), and (30) convert Eq.(11) into a time-invariant system while preserving the stability properties. The unit-circle stability criteria is applied for Floquet multipliers (eigenvalues of $\mathbf{\Phi}(T)$) and their squares (eigenvalues of $\mathbf{\Phi}(2T)$), while for the corresponding eigenvalues of $\mathbf{C}$, $\mathbf{R}$, and $\bar{\mathbf{R}}$ (characteristic exponents) the left half-plane stability criteria is used.

3.2. *Example*: *Delayed Mathieu Equation*

As an illustrative example of the use of LFT, consider the delayed Mathieu's equation[66]

$$\ddot{x}(t) + (a + b\cos t)x(t) = cx(t - 2\pi). \tag{34}$$

The CSCTA was applied to Eq.(34) in Ref.52 to transform the DDE into an approximate ODE representation of the system given by

$$\dot{\mathbf{y}}(t) = \begin{bmatrix} \begin{bmatrix} 0 & 1 \\ -a - b\cos t & 0 \end{bmatrix} & \mathbf{0}_q & \cdots & \mathbf{0}_q & \begin{bmatrix} 0 & 0 \\ c & 0 \end{bmatrix} \\ & \frac{1}{\pi}\left[\mathbb{D}^{\,(3,2m)}\right] & & & \end{bmatrix} \mathbf{y}(t). \tag{35}$$

Consider a specific set of parameters $(a, b, c) = (1.5, 0.1, 0.1)$ that results in a stable location shown on the stability chart in Fig.5, and assume $m = 20$ collocation points are used. CSCTA results in a pair of complex conjugate squares of Floquet multipliers $(-0.4296 \pm 0.2250i)$ and a number of inaccurate multipliers of the matrix $\mathbf{\Phi}(2T)$ clustered around zero within the unit circle shown in Fig.6(a). This set of inaccurate multipliers are mapped into a set of inaccurate eigenvalues of $\mathbf{R}$ (characteristic exponents) as shown in Fig.6(b). Hence, a reduced order $2T$-periodic LFT matrix is computed from Eq.(33).

We can get the expressions for the elements of the RLFT matrix as a Fourier series with 5 harmonics by evaluating the product of the reduced STM and the

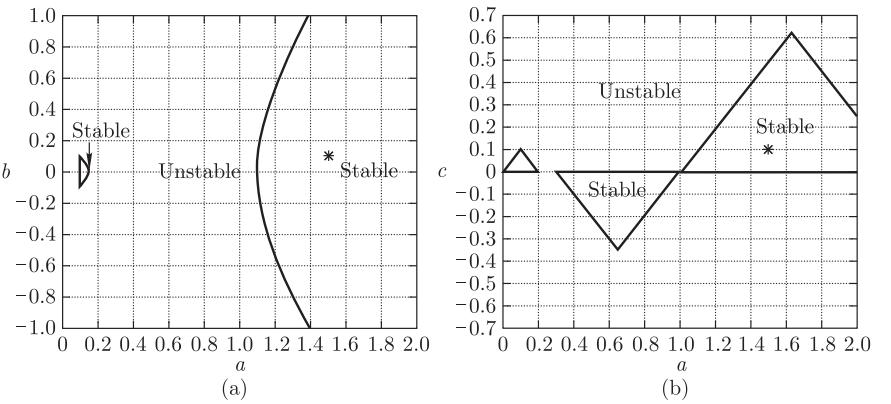

Fig. 5. The stability charts for the delayed Mathieu's equation for (a) $c = 0.1$ in the (a, b) plane also obtained in Ref.52 and (b) $b = 0.1$ in the (a, c) plane. The asterisk shows the stable point $(a, b) = (a, c) = (1.5, 0.1)$.

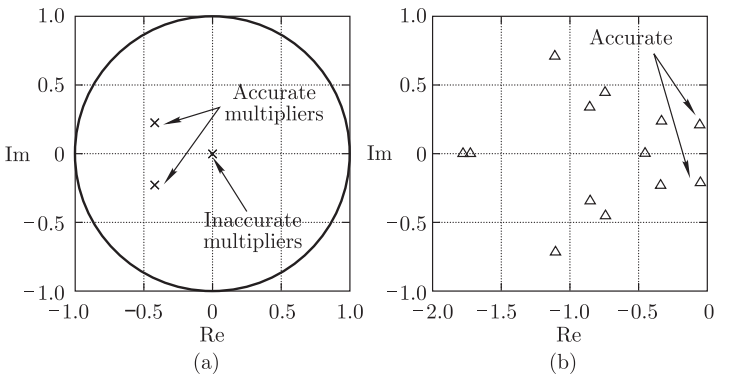

Fig. 6. In the first row, (a) the squares of Floquet multipliers and (b) the characteristic exponents of the LF-transformed system are given. Note the sets of accurate and inaccurate multipliers and exponents.

matrix exponential at the intermediate points of the interval $[0, 2T]$. These entries are also plotted in Fig.7. The constant reduced system in terms of 2-dimensional vector $\mathbf{w}(t)$ is given by

$$\dot{\mathbf{w}}(t) = \begin{bmatrix} -0.04799 & 0.1681 \\ -0.2665 & -0.06717 \end{bmatrix} \mathbf{w}(t) \tag{36}$$

whose eigenvalues are $-0.05758 \pm 0.2115i$.

In Fig.8, the responses of the dominant modes of the reduced order system transformed by the RLFT matrix $\bar{\mathbf{Q}}(t)$ (i.e., the $\mathbf{w}(t)$ vector back-transformed to $\mathbf{y}$ coordinates) are compared to the corresponding numerically obtained dominant modes of the full time-periodic ODE system defined in Eq.(35) (i.e., the first two components of the $\mathbf{y}(t)$ vector) and the two states of the DDE in Eq.(34) (i.e., $x(t)$

and $\dot{x}(t)$). To compare the three responses, it is essential to choose equivalent initial conditions as explained in Ref.53. For the time series shown in Fig.8, the initial conditions are

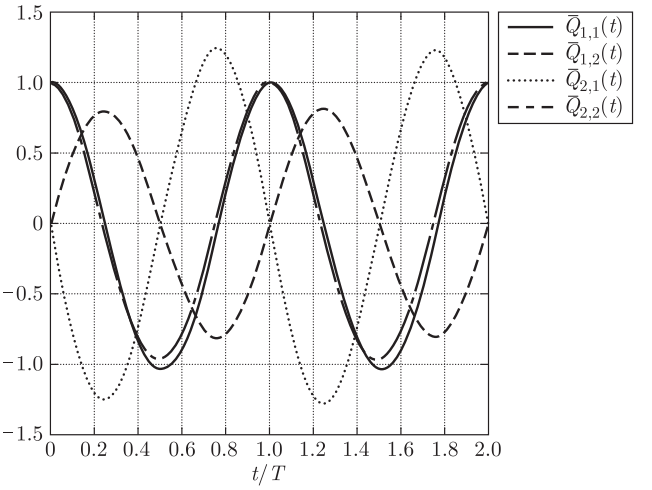

Fig. 7. Elements of the 2×2 reduced order LFT matrix for the stable point $(a, b) = (1.5, 0.1)$ on the stability chart in Fig.5.

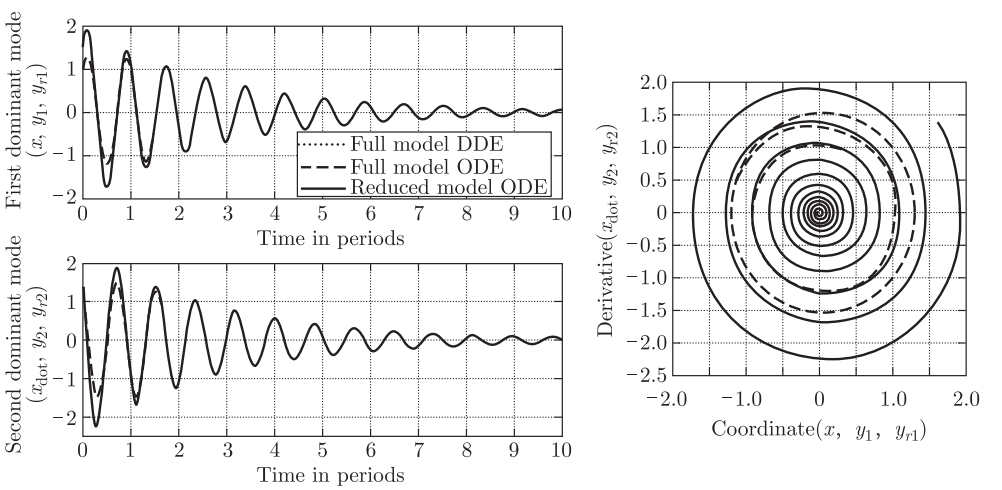

Fig. 8. The time series and the phase plane of the two dominant mode responses obtained by integrating the time-periodic DDE 34 (dotted, matches the dashed line), the full size time-periodic ODE 35 (dashed), and the reduced constant system 36 back-transformed by the reduced LFT (solid) are shown.

$$\mathbf{y}(0) = [\underbrace{1,\ 1, \cdots, 1}_{2m \text{ times}}]^T,$$
$$\mathbf{w}(0) = [1.5932,\ 1.4091]^T, \tag{37}$$
$$\phi(t) = [1,\ 1]^T \text{ for } t \in [-\tau, 0].$$

It can be seen that the responses of the reduced constant system with the RLFT applied do not match those of the time-periodic DDE and the time-periodic ODE system for a short period of time in the beginning but become almost indistinguishable later in time. This short interval is the time it takes the exponential solutions corresponding to the neglected characteristic exponents to completely die out.

4. Feedback Control of Periodic Delayed Systems

Many strategies have been utilized to control time-delayed systems or to design delayed feedback control laws for non-delayed systems in the case that the current states are unavailable for feedback. For linear time-invariant control systems with delay, the stabilization problem is to design a control law such that all of the closed-loop poles (eigenvalues) lie in the left-half plane. If pole placement is desired to ensure a specified response, however, one is faced with the problem that infinitely many poles should be specified, while the number of control parameters (gains) is finite. One strategy is to assign the place of the dominant poles only or to specify only the spectral abscissa[9,38]. An alternative strategy is to use an infinite (or large) number of control gains to control all (or many) of the poles[7]. Two techniques to implement this strategy include the use of distributed delays in the controller (in which the kernel function of the distributed delay serves as an infinite-dimensional vector of control gains) or by allowing the control gains to be time-periodic in which their Fourier coefficients form a set of infinitely many control parameters. While the stabilization of non-delayed systems by means of periodic control gains has been the focus of recent papers (e.g., Refs.82, 83), the combined effect of feedback delay and time-periodic control gains results in time-periodic DDEs, for which the stability analysis requires the use of the infinite-dimensional Floquet theory. This technique was utilized in Ref.47, for instance, in which two Fourier coefficients for the periodic control gains were utilized.

Yet a third strategy for delayed feedback control is that of finite spectrum assignment, in which the resulting closed-loop system has only a finite number of poles that can be assigned arbitrarily and thus requires only a finite number of control gains to be specified. Two techniques to implement this strategy include the use of a feedback based on a prediction of the state with distributed delay, e.g., Refs.14, 32, 34, 35, and also utilizing a special case of periodic controllers call "act-and-wait control" where the feedback term is switched on and off periodically in time[42–44].

The advantage in this control strategy is that if the switch-off (waiting) period is longer than the feedback delay, then the system can be transformed to a discrete map of finite dimension thus presenting a finite spectrum assignment problem. In Ref.7, several examples showed that an unstable process can be stabilized by the application of the act-and-wait concept where the traditional constant gain controllers cannot stabilize the system.

The remainder of this section will outline several strategies for the use of the CSCTA and RLFT methods can help to reduce a (possibly time-periodic) nonlinear delayed system with linear and/or nonlinear feedback control into a form more conducive for the application of many of the techniques for control of delayed systems discussed above and allow the application of standard tools for control design of LTI systems. While control design based on finite difference discretization of the infinitesimal generator has been demonstrated in Ref.37 and the LFT has been utilized for the control of time-periodic non-delayed systems[72,84–91], the use of CSCTA and RLFT have thus far not been investigated for their application in control design for delayed periodic systems or for delayed feedback control using periodic gains of non-delayed time-invariant systems. Therefore, the remainder of this section offers a few ideas for implementation of these strategies.

4.1. *Formulation*

Consider the q-dimensional nonlinear (quasi linear) system with a single point delay given by

$$\dot{\mathbf{x}} = \mathbf{A}_1(t)\mathbf{x}(t) + \mathbf{A}_2(t)\mathbf{x}(t-\tau) + \mathbf{f}(\mathbf{x}(t), \mathbf{x}(t-\tau), t) + \mathbf{B}(t)\mathbf{u}(t) \tag{38}$$

in which $\mathbf{A}_1(t), \mathbf{A}_2(t), \mathbf{B}(t)$, and the purely nonlinear vector function $\mathbf{f}(\cdot)$ are periodic in t with period T. Application of CSCTA using m Chebyshev collocation points transforms Eq.(38) into the periodic nonlinear ODE system

$$\dot{\mathbf{y}} = \hat{\mathbf{A}}(t)\mathbf{y} + \hat{\mathbf{f}}(\mathbf{y}, t) + \hat{\mathbf{B}}(t)\mathbf{u}(t), \quad \hat{\mathbf{B}}(t) = \begin{bmatrix} \mathbf{B}(t) \\ 0 \\ \vdots \\ 0 \end{bmatrix} \tag{39}$$

where $\hat{\mathbf{A}}(t)$ and $\hat{\mathbf{f}}(\cdot)$ are time-periodic analogues of those in Eq.(7), and $\mathbf{y}$ is an mq-dimensional vector. At this point a full-state feedback control law can be designed using a linear, nonlinear, or a combined linear/nonlinear controller with periodic control gains as

$$\mathbf{u}(t) = -\mathbf{K}(t)\mathbf{y} + \mathbf{k}(\mathbf{y}, t) \tag{40}$$

where $\mathbf{K}(t)$ and the purely nonlinear function $\mathbf{k}(\cdot)$ are periodic in t with period T and can thus be expressed using finite Fourier series with coefficients to be specified.

Note that the form of the feedback control law in $\mathbf{y}(t)$ translates into a distributed delay control law in $\mathbf{x}(t)$, i.e.,

$$\mathbf{u}(t) = -\int_{-\tau}^{0} \bar{\mathbf{K}}(t,\theta)\mathbf{x}(t+\theta)d\theta + \int_{-\tau}^{0} \bar{\mathbf{k}}(\mathbf{x}(t+\theta),t,\theta)d\theta \tag{41}$$

where Clenshaw-Curtis quadrature is used to obtain the gain matrix $\mathbf{K}(t)$ and the nonlinear control term $\mathbf{k}(\cdot)$ from $\bar{\mathbf{K}}(t)$ and $\bar{\mathbf{k}}(\cdot)$. Note that the control law in Eqs.(40) and (41) includes feedback of the current state $\mathbf{x}(t)$. If sensor and/or actuator delays make the current and delayed states $\mathbf{x}(t+\theta)$, $-\tau_c < \theta \leq 0$ unavailable for feedback, however, then the appropriate weights in Eq.(41) must be set to zero. Alternatively, the control input can be changed to $\mathbf{u}(t-\tau_c)$ or output feedback can be employed.

Consider the linear versions of Eqs.(38)–(41) in which we have to design the matrix $\mathbf{K}(t)$ such that the closed-loop system is asymptotically stable. We do not require both the uncontrolled system and the control law to have delay and periodic coefficients, but we assume that each property shows up in at least one place. Note that a large number of control gains are available, both from the discretization of the distributed delay feedback control and from the Fourier series expansion (up to any desired order) of the periodic coefficients of $\mathbf{K}(t)$, to control a large number of the closed-loop poles. Our assumption of controllability applies only to $(\mathbf{A}_1(t), \mathbf{B}(t))$ in Eq.(38), because in fact the pair $(\hat{\mathbf{A}}(t), \hat{\mathbf{B}}(t))$ may not be controllable even if the pair $(\mathbf{A}_1(t), \mathbf{B}(t))$ is originally controllable as shown in Ref.37. Practically, this is not a problem since all we require is to control the current state $\mathbf{y}_1(t) = \mathbf{x}(t)$ and not $\mathbf{y}_i(t)$, $i = 2, \ldots, m$ as these are simply delayed states. Hence, for pole placement we typically cannot place all mq poles even if the matrices $\hat{\mathbf{A}}, \hat{\mathbf{B}}, \mathbf{K}$ are time-invariant. Again, this is not a concern as long as the poles being placed include the dominant ones.

We now outline three possible strategies for determining the gain matrix $\mathbf{K}(t)$ in the linear problem. First, the stability of the closed-loop response may be investigated in the parameter space of available control gains using Floquet theory, including the possibility of optimization of the control gains by minimizing the spectral radius which must be less than unity for asymptotic stability[37]. This strategy does not use either CSCTA or RLFT. We note that rather than obtaining the monodromy matrix associated with the closed-loop matrix $(\hat{\mathbf{A}}(t) - \hat{\mathbf{B}}(t)\mathbf{K}(t))$, other numerical techniques such as Chebyshev collocation[18] and semidiscretization[7] may be directly applied to the closed-loop DDE to more efficiently generate an approximation to the infinite-dimensional monodromy operator. This strategy was employed in Refs.49–51 as well as in Ref.47 in which the monodromy operator was approximated symbolically via Chebyshev polynomial expansion[17,92] in terms of constant and periodic (with unknown Fourier coefficients) control gains.

The second strategy utilizes CSCTA but not RLFT. It uses optimal (time-

varying LQR) control to minimize the cost function

$$J = \frac{1}{2}\mathbf{y}^T(t_f)\mathbf{S}\mathbf{y}(t_f) + \frac{1}{2}\int_0^{t_f} \left(\mathbf{y}^T(t)\mathbf{Q}(t)\mathbf{y}(t) + \mathbf{u}^T(t)\mathbf{R}(t)\mathbf{u}(t)\right) dt, \tag{42}$$

where $\mathbf{Q}(t)$ and $\mathbf{R}(t)$ are symmetric positive definite T-periodic matrices, by directly solving the time-periodic Riccati equation

$$\dot{\mathbf{P}}(t) = -\left(\hat{\mathbf{A}}^T(t)\mathbf{P}(t) + \mathbf{P}(t)\hat{\mathbf{A}}(t) + \mathbf{Q}(t)\right) + \mathbf{P}(t)\hat{\mathbf{B}}(t)\mathbf{R}^{-1}(t)\hat{\mathbf{B}}^T(t)\mathbf{P}(t) \tag{43}$$

backwards in time from the final value $\mathbf{P}(t_f) = \mathbf{S}$. The control gain is then obtained as

$$\mathbf{K}(t) = \mathbf{R}^{-1}(t)\hat{\mathbf{B}}^T(t)\mathbf{P}(t). \tag{44}$$

Note, however, that solving the large-dimensional Riccati equation is computationally intensive and may not be practical in applications. If $\hat{\mathbf{A}}$, $\hat{\mathbf{B}}$, $\mathbf{Q}$, and $\mathbf{R}$ are constant and $\mathbf{S} = \mathbf{0}$, however, then the much simpler algebraic LQR problem can be solved for the case where $t_f \to \infty$.

The third strategy for obtaining a non-delayed control law is adopted from Refs.87, 90 and involves use of both CSCTA and RLFT as well as pole-placement for LTI systems. Again, consider the control problem associated with the linear parts of Eqs.(38)–(41) where the output matrix $\mathbf{C}(t) = \mathbf{I}_{mq}$. Application of RLFT with q dominant modes to $\dot{\mathbf{y}} = \hat{\mathbf{A}}(t)\mathbf{y} + \hat{\mathbf{B}}(t)\mathbf{u}(t)$ yields

$$\dot{\mathbf{w}}(t) = \bar{\mathbf{R}}\mathbf{w}(t) + (\hat{\mathbf{T}}^T\hat{\mathbf{T}})^{-1}\hat{\mathbf{T}}^T\mathbf{Q}^{-1}(t)\hat{\mathbf{B}}(t)\mathbf{u}(t). \tag{45}$$

Recall from Section 3 that $\mathbf{T}^T\mathbf{Q}(t) = \bar{\mathbf{Q}}(t)\mathbf{T}^T$. It can be shown by solving for $\mathbf{Q}^T(t)\mathbf{T}$=$\hat{\mathbf{T}}(\hat{\mathbf{T}}^T\hat{\mathbf{T}})^{-1}\bar{\mathbf{Q}}^T(t)$, taking the transpose, and pre- and post-multiplying the result by $\bar{\mathbf{Q}}^{-1}(t)$ and $\mathbf{Q}^{-1}(t)$, respectively, that the projection $(\hat{\mathbf{T}}^T\hat{\mathbf{T}})^{-1}\hat{\mathbf{T}}^T\mathbf{Q}^{-1}(t)$ reduces to $\bar{\mathbf{Q}}^{-1}(t)\mathbf{T}^T$. Also recalling the form of $\hat{\mathbf{B}}(t)$ in Eq.(39), equation (45) is expressed in terms of the RLFT matrix $\bar{\mathbf{Q}}(t)$ as

$$\dot{\mathbf{w}}(t) = \bar{\mathbf{R}}\mathbf{w}(t) + \bar{\mathbf{Q}}^{-1}(t)\mathbf{B}(t)\mathbf{u}(t). \tag{46}$$

Now consider an auxiliary system of the form

$$\dot{\bar{\mathbf{w}}}(t) = \bar{\mathbf{R}}\bar{\mathbf{w}}(t) + \bar{\mathbf{B}}\mathbf{v}(t) \tag{47}$$

where $\bar{\mathbf{B}}$ is an arbitrary constant matrix with the same order and rank as $\bar{\mathbf{Q}}^{-1}(t)\mathbf{B}(t)$ such that $(\bar{\mathbf{R}}, \bar{\mathbf{B}})$ is a controllable pair. The state feedback control law $\mathbf{v}(t) = -\bar{\mathbf{K}}\bar{\mathbf{w}}(t)$ can be designed by applying pole placement or optimal control theory such that equation (47) is asymptotically stable. Defining $\mathbf{e}(t) = \mathbf{w}(t) - \bar{\mathbf{w}}(t)$, the error dynamics from Eqs.(46) and (47) are given as

$$\dot{\mathbf{e}}(t) = (\bar{\mathbf{R}} - \bar{\mathbf{B}}\bar{\mathbf{K}})\mathbf{e}(t) + \bar{\mathbf{Q}}^{-1}(t)\mathbf{B}(t)\mathbf{u}(t) - \bar{\mathbf{B}}\mathbf{v}(t). \tag{48}$$

Assuming $\mathbf{B}(t)$ is a rectangular matrix, the control law for $\mathbf{u}(t)$ is found by using least squares to minimize the norm of the time-varying term $\bar{\mathbf{Q}}^{-1}(t)\mathbf{B}(t)\mathbf{u}(t)-\bar{\mathbf{B}}\mathbf{v}(t)$ along with the above control law for $\mathbf{v}(t)$ as

$$\mathbf{u}(t) = -\mathbf{B}^{\dagger}(t)\bar{\mathbf{Q}}(t)\bar{\mathbf{B}}\bar{\mathbf{K}}\mathbf{w}(t) \tag{49}$$

where $\mathbf{B}^{\dagger}(t)$ is the least squares inverse of $\mathbf{B}(t)$. Substituting $\mathbf{w}(t) = \bar{\mathbf{Q}}^{-1}(t)\mathbf{x}(t)$ into Eq.(49) provides the non-delayed feedback control law $\mathbf{u}(t) = -\mathbf{K}(t)\mathbf{x}(t)$ where

$$\mathbf{K}(t) = \mathbf{B}^{\dagger}(t)\bar{\mathbf{Q}}(t)\bar{\mathbf{B}}\bar{\mathbf{K}}\bar{\mathbf{Q}}^{-1}(t). \tag{50}$$

As is discussed in Ref.88, due to use of the least squares inverse asymptotic stability of the closed-loop dynamics is not guaranteed and one must search for the optimal $\bar{\mathbf{B}}$ matrix that provides the best response. Alternatively, use of a backstepping strategy as detailed in Ref.88 does guarantee asymptotic stability for underactuated systems. Also, as is explained in Refs.72, 84, 88–90 the strategy for computing $\bar{\mathbf{Q}}^{-1}(t)$ involves finding the STM $\mathbf{\Psi}(t)$ associated with the adjoint system

$$\dot{\mathbf{s}}(t) = -\hat{\mathbf{A}}^{T}(t)\mathbf{s}(t) \tag{51}$$

and using the relationships $\mathbf{\Phi}^{-1}(t) = \mathbf{\Psi}^{T}(t)$ and

$$\mathbf{Q}^{-1}(t) = \left[\mathbf{\Phi}e^{-\mathbf{R}t}\right]^{-1} = e^{\mathbf{R}t}\mathbf{\Phi}^{-1}(t) = e^{\mathbf{R}t}\mathbf{\Psi}^{T}(t). \tag{52}$$

Hence $\bar{\mathbf{Q}}^{-1}(t)$ is a projection of $\mathbf{Q}^{-1}(t)$ that satisfies $\bar{\mathbf{Q}}^{-1}(t)\mathbf{T}^{T} = \mathbf{T}^{T}\mathbf{Q}^{-1}(t)$, and hence $\bar{\mathbf{Q}}^{-1}(t) = \mathbf{T}^{T}\mathbf{Q}^{-1}(t)\mathbf{T} = (\mathbf{Q}^{-1}(t))_{11}$. Again, however, it is impractical to compute the full $\mathbf{Q}^{-1}(t)$ in the first place. A formula for $\bar{\mathbf{Q}}^{-1}(t)$ analogous to that for $\bar{\mathbf{Q}}(t)$ in Section 3 is

$$\bar{\mathbf{Q}}^{-1}(t) = e^{\mathbf{R}_{11}t}\mathbf{\Psi}_{11}^{T}(t). \tag{53}$$

Additional strategies for control of time-periodic systems are discussed in Refs.87, 90 which could be used for control of linear periodic DDEs after employing CSCTA and RLFT include output feedback and an observer-based controller. Possible strategies for designing the full nonlinear control law in Eq.(40) also involve use of CSCTA and RLFT applied to Eq.(39) which yields (assuming $T = \tau$)

$$\begin{aligned}\dot{\mathbf{w}}(t) &= \bar{\mathbf{R}}\mathbf{w}(t) + \bar{\mathbf{Q}}^{-1}(t)\mathbf{T}^{T}\left[\hat{\mathbf{f}}(\mathbf{y}(t),t) + \hat{\mathbf{B}}(t)\mathbf{u}(t)\right] \\ &= \bar{\mathbf{R}}\mathbf{w}(t) + \bar{\mathbf{Q}}^{-1}(t)\left[\mathbf{f}\left(\bar{\mathbf{Q}}(t)\mathbf{w}(t), \bar{\mathbf{Q}}(t)\mathbf{w}(t-\tau), t\right) + \mathbf{B}(t)\mathbf{u}(t)\right].\end{aligned} \tag{54}$$

Hence, it is seen that the combined use of CSCTA and RLFT allows for the linear part of the uncontrolled periodic DDE to be expressed in an equivalent time-invariant and non-delayed form which preserves the dominant characteristic exponents, while the nonlinear part of the transformed system retains both time delay and periodic coefficients. Hence, various reduced order controllers[93], chaos controllers[73,85,86], or bifurcation controllers[72] for nonlinear periodic systems could now be applied after modification to account for possible time delays in the nonlinear part by designing both the linear and nonlinear controls in Eq.(40). We also

point out that if the nonlinear DDE is uncontrolled with critical Floquet multipliers/exponents, then the strategy for invariant-manifold based order reduction used in Refs.70, 71 becomes an alternative for center manifold reduction for nonlinear constant or periodic DDEs[76–80].

4.2. *Delayed State Feedback Control of the Delayed Mathieu Equation*

Consider the controlled delayed Mathieu equation

$$\begin{gathered}\ddot{x} + (0.2 + 0.1\cos 2\pi t)x(t) = 0.5x(t-1) + u(t), \\ (x, \dot{x}) = (1, 0),\ -1 \le t \le 0.\end{gathered} \tag{55}$$

Following the first strategy described in Section 4.1, the monodromy operator of the uncontrolled system is approximated and is found to have a spectral radius larger than unity such that the uncontrolled system is unstable. In order to obtain the asymptotic stability of the controlled system, we design a delayed state feedback controller with a periodic gain matrix in which each gain component is expressed in a 3-term Fourier series with unknown coefficients to be determined as

$$\begin{aligned}u(t) = &-(k_{11} + k_{12}\cos 2\pi t + k_{13}\sin 2\pi t)x(t-1) \\ &-(k_{21} + k_{22}\sin 2\pi t + k_{23}\cos 2\pi t)\dot{x}(t-1).\end{aligned} \tag{56}$$

Note that the period and delay are the same as in Eq.(55), although this is not necessary. Any relationship between the delays in the plant and control law are acceptable when using the multi-interval version of CSCTA in Eq.(12), while the periods of the coefficients should be rationally related in order for Floquet theory to be applied using the fundamental period of the closed-loop system.

First, we set $k_{12} = k_{13} = k_{22} = k_{23} = 0$ and find the stable region in the k_{11}-k_{21} parameter space. For this purpose, the monodromy operator $\mathbf{U}$ is approximated using the Chebyshev collocation method[18]. The set of the points in the k_{11}-k_{21} parameter space for which the spectral radius of $\mathbf{U}$ lies on the circumference of the unit circle forms the stability boundary. Starting from a unity spectral radius and plotting contours for gradually decreasing spectral radii, the (k_{11}, k_{21}) location corresponding to the minimum spectral radius can be obtained. The optimum set of the first pair of the control gains is $(k_{11}, k_{21}) = (0.40, 0.35)$ which corresponds to the spectral radius $\rho = 0.54577$. Next, the optimal values obtained for k_{11} and k_{21} are held constant with $k_{13} = k_{23} = 0$ while the stable region in the k_{12}-k_{22} parameter space is found as well as the values of k_{12} and k_{22} that correspond to the minimum spectral radius for the new controlled system. The optimum set of the second pair of the control gains, i.e., $(k_{12}, k_{22}) = (-0.33, -0.06)$, corresponds to the spectral radius $\rho = 0.52154$. Finally, the optimum values obtained for k_{11}, k_{21}, k_{12}, and k_{22} are held constant while the stability region in the k_{13}-k_{23} parameter space is found as well as their optimum values. The minimum spectral radius is $\rho_{\text{opt}} = 0.51977$ which corresponds to $(k_{13}, k_{23}) = (0.03, -0.06)$. Altogether, the optimal set of the

control gains is $(k_{11}, k_{21}, k_{12}, k_{22}, k_{13}, k_{23}) = (0.40, 0.35, -0.33, -0.06, 0.03, -0.06)$. These results are obtained using 150 Chebyshev collocation points and a 500×500 meshgrid for each parameter space. The optimum control gains are shown with • in the stability diagrams shown in Fig.9. Figure 10 shows the uncontrolled response of the system in Eq.(55), the controlled response using the optimal constant control law, and that using the optimal full 6-term periodic control law, along with the corresponding control efforts. The simulated results indicate that when the optimal values of the control gains are used, the closed-loop response has less settling time due to a greater effective damping, and that k_{11} and k_{21} have a more significant role in the convergence speed.

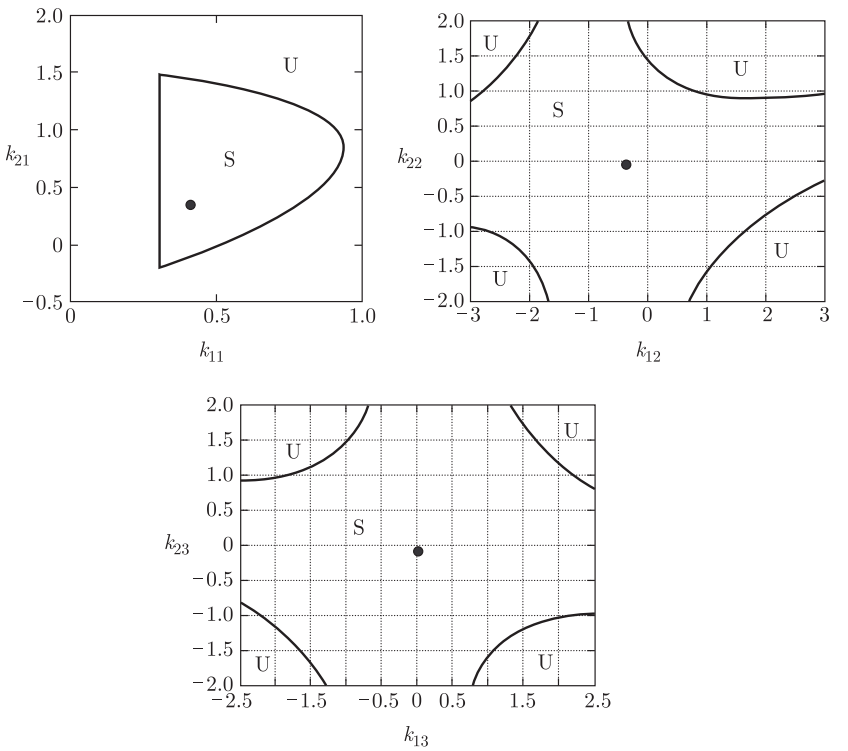

Fig. 9. The stable (labeled with S) and unstable (labeled with U) regions in different parameter spaces. The optimal control pairs are shown with •.

Note that although semi-discretization can also be utilized for the optimum control design, because of the spectral convergence in the Chebyshev collocation method, we have only shown the results obtained by the Chebyshev collocation method. We also note that the above example only illustrates the first of the three control strategies discussed in Section 4.1. For future work it is planned to directly compare the advantages and disadvantages of these techniques.

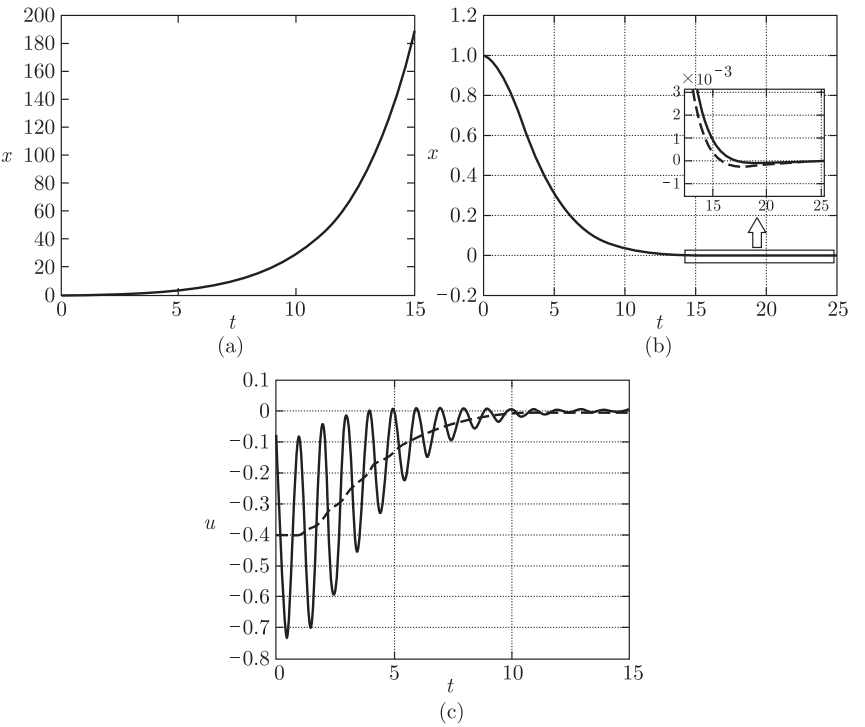

Fig. 10. (a) the uncontrolled response for Eq.(55), (b) the controlled response for Eq.(55) with the constant gain control law (thin line) versus that with the full 6-term periodic control law (thick line), and (c) the control effort corresponding to the constant gain control law (thin line) versus that corresponding to the full 6-term periodic control law (thick line).

5. Stochastic State, Parameter, and Delay Estimation

5.1. *Formulation*

In a general stochastic estimation problem it is assumed that the form of the model is known only approximately due to imperfect knowledge of the dynamical model that describes the motion and/or imperfect knowledge of parameters. The goal is to obtain the best estimate of the state as well as of model parameters based on measured data that has a random component due to observation errors[94]. In addition, a second source of stochastic excitation typically appears in the state dynamics as so-called process noise which can be either additive or multiplicative[95]. Similarly, a stochastic estimation problem in a delayed system aims to find the best estimate of the state and parameters of a stochastically-excited delayed system from measured data that contains an additive random observation error.

There has been little work reported in the literature concerning stochastic estimation or parameter identification for time delay systems. Among those reported, most are limited to an identifiability analysis of parameters[24,25,28]. Orlov et al.[25]

developed an adaptive parameter identifier for linear dynamic systems with finitely many lumped delays in the state vector and control input to simultaneously identify the system parameters and the delay. Mann et al.[29] examined the experimental data with empirical Floquet theory and principle orthogonal decomposition to estimate the parameters of a linear time-periodic delayed system from a reduced order map of the system. Tang and Guan[27] studied the problem of estimating time delay and parameters of time-delayed first-order scalar chaotic systems by first converting the problem into an optimization problem with a suitable objective function and applying a particle swarm optimization algorithm. Sun and Yang[26] exploited chaos synchronization for parameter identification of chaotic delayed systems with varying time delay through using an adaptive feedback controller based on the Razumikhin condition and the invariance principle of functional differential equations in the framework of Lyapunov-Krasovskii theory. Also, parameter estimation of nonlinear time-varying DDEs with constant delay from fully and partially available data has been studied by Deshmukh[30] wherein an ideal case of parameter linearity with no external random disturbance was considered. Chebyshev spectral collocation is used to convert the delayed dynamic system (model) into an algebraic system with unknown parameters, and subsequently a standard least-squares optimization is employed to find the solution for the unknown parameters. Other studies have investigated parameter identification in delayed chaotic systems[26,27]. While in all of the aforementioned studies, the critical role of measurement noise and model uncertainties are ignored, in Refs.22, 23 the problem of optimal filtering in stochastic time delay systems was considered by designing an optimal finite-dimensional filter.

It is clear that the problem of identifying the unknown parameters of a stochastic time-delayed system from the time series response is still open to novel efficient techniques. Here, we present a novel approach for state, delay, and parameter identification of time-varying DDEs through exploiting continuous time approximation and optimal filtering. Specifically, optimal estimation of stochastic linear and nonlinear constant and periodic DDEs having time-varying coefficients and possibly unknown delay from possibly incomplete measurements is studied. In this technique, which is outlined below, the stochastic delay differential equation is first discretized with a set of ODEs using CSCTA. Then the estimation problem in the resulting stochastic ODE system is represented as an optimal filtering problem using a state augmentation technique. Finally, using extended Kalman-Bucy (EKB) filters, the unknown state, delay, and parameters of a nonlinear DDE are estimated from a noise-corrupted, possibly incomplete measurement of the states.

The estimation problem of a delayed system in its general form can be formulated as an optimal continuous-time filtering problem in the form of a set of Itô stochastic delay differential equations as

$$\begin{aligned} d\mathbf{x}(t) &= \mathbf{f}(\mathbf{x}(t), \mathbf{x}(t-\tau), \mathbf{a}(t), t)dt + \mathbf{G}(\mathbf{x}(t), t)d\boldsymbol{\beta}(t), \\ d\mathbf{z}(t) &= \mathbf{h}(\mathbf{x}(t), \mathbf{x}(t-\tau), t)dt + \mathbf{J}(t)d\boldsymbol{\eta}(t) \end{aligned} \tag{57}$$

where $\boldsymbol{\beta}(t)$ and $\boldsymbol{\eta}(t)$ are independent Brownian motion additive stochastic processes with $E[d\boldsymbol{\beta}(t)] = E[d\boldsymbol{\eta}(t)] = 0$, $E[d\boldsymbol{\beta}(t)d\boldsymbol{\beta}^T(t)] = \mathbf{Q}dt$, $E[d\boldsymbol{\eta}(t)d\boldsymbol{\eta}^T(t)] = \mathbf{R}dt$, $E[\cdot]$ represents the expectation operator, and $\mathbf{a}(t)$ represents a vector of parameters to be estimated. Note that the process noise is multiplicative if $\mathbf{G}(\cdot)$ depends on $\mathbf{x}(t)$ and additive if it does not depend on $\mathbf{x}(t)$. Alternatively, the estimation problem for additive noise problems may be formulated in terms of the stationary zero-mean Gaussian white noise processes formally defined as $\mathbf{v}(t) = d\boldsymbol{\beta}(t)/dt$, $\mathbf{w}(t) = d\boldsymbol{\eta}(t)/dt$ and measurement process $\mathbf{y}(t) = d\mathbf{z}(t)/dt$ as

$$\begin{aligned}\dot{\mathbf{x}}(t) &= \mathbf{A}_1(\mathbf{a}(t),t)\mathbf{x}(t) + \mathbf{A}_2(\mathbf{a}(t),t)\mathbf{x}(t-\tau)\\ &\quad +\mathbf{g}(\mathbf{x}(t),\mathbf{x}(t-\tau),\mathbf{a}(t),t) + \mathbf{G}(t)\mathbf{v}(t),\\ \mathbf{y}(t) &= \mathbf{h}(\mathbf{x}(t),\mathbf{x}(t-\tau),t) + \mathbf{J}(t)\mathbf{w}(t)\end{aligned} \tag{58}$$

where $\mathbf{G}(t)$ is assumed to be independent of $\mathbf{x}(t)$, $\mathbf{v}(t)$, and $\mathbf{w}(t)$ are assumed to be both mutually independent and independent from the state and observation with constant covariance matrices of $\mathbf{Q}$ and $\mathbf{R}$, respectively, i.e., $\mathbf{v} \sim N(\mathbf{0},\mathbf{Q})$ and $\mathbf{w} \sim N(\mathbf{0},\mathbf{R})$, and the linear part of the process model is shown explicitly in the $\mathbf{A}_1$ and $\mathbf{A}_2$ matrices. Note that $\mathbf{a}(t)$ can be a constant vector and it is assumed to be time varying here only to keep the generality of the notation.

The filtering problem can be represented in the context of parameter estimation, using the so-called state augmentation method, in which the parameter vector $\mathbf{a}$ (now assumed to be constant) is included with the state vector while being constrained to have a zero rate of change, i.e.,

$$\begin{aligned}\left\{\begin{array}{c}\dot{\mathbf{x}}(t)\\ \dot{\mathbf{a}}(t)\end{array}\right\} &= \left\{\begin{array}{c}\mathbf{A}_1(\mathbf{a},t)\mathbf{x} + \mathbf{A}_2(\mathbf{a},t)\mathbf{x}_\tau + \mathbf{g}(\mathbf{x},\mathbf{x}_\tau,\mathbf{a},t)\\ \mathbf{0}\end{array}\right\} + \left\{\begin{array}{c}\mathbf{G}(t)\\ \mathbf{0}\end{array}\right\}\mathbf{v}(t),\\ \mathbf{y}(t) &= \mathbf{h}(\mathbf{x},\mathbf{x}_\tau,t) + \mathbf{J}(t)\mathbf{w}(t)\end{aligned} \tag{59}$$

where $\mathbf{x}_\tau$ denotes $\mathbf{x}(t-\tau)$. The purpose of the optimal continuous-time filtering problem is to recursively obtain estimates of the states and parameters from the mean, median, or mode of the time-varying conditional probability density

$$P\left(\mathbf{x}(t)\middle|\left\{\mathbf{y}(\rho):\ 0 \le \rho \le t\right\}\right). \tag{60}$$

The parameter vector $\mathbf{a}(t)$ is assumed to initially have a Gaussian distribution with mean $\mathbf{a}_0$ and covariance $\mathbf{P}_0$. Therefore, the augmented state method along with optimal filtering problem provides a pertinent approach for simultaneous estimate of the state and parameters of a nonlinear system. However, in order for the approach to be applicable, the DDE of the system needs to be expressed as a system of ODEs

using CSCTA. This results in the system of ODEs given by

$$\begin{Bmatrix} \dot{\mathbf{Y}}(t) \\ \dot{\mathbf{a}}(t) \end{Bmatrix} = \left\{ \begin{bmatrix} \mathbf{A}_1(\mathbf{a},t) & \mathbf{0}_{n\times n} & \cdots & \mathbf{0}_{n\times n} & \mathbf{A}_2(\mathbf{a},t) \\ & & \frac{2}{\tau}\left[\mathbb{D}^{(n+1:nm,:)}\right] & & \\ & & & & \mathbf{0}_{r\times 1} \end{bmatrix} \mathbf{Y}(t) + \begin{bmatrix} \mathbf{g}(\mathbf{Y}_1(t), \mathbf{Y}_m(t), \mathbf{a}, t) \\ \mathbf{0}_{n(m-1)\times 1} \end{bmatrix} \right\} + \left\{ \begin{bmatrix} \mathbf{G}(t) \\ \mathbf{0}_{n(m-1)\times 1} \end{bmatrix} \right\} \mathbf{v}(t), \tag{61}$$

$$\mathbf{y}(t) = \mathbf{h}(\mathbf{Y}_1(t), \mathbf{Y}_m(t), t) + \mathbf{J}(t)\mathbf{w}(t)$$

where $\mathbf{Y}(t)$ is now used for the expanded state vector since $\mathbf{y}(t)$ denotes the measurement.

Note that since the linear matrix in Eq.(61) is a function of the augmented states, even if the delay system and the resulting approximated ODE are linear ($\mathbf{g} = \mathbf{0}$), the optimal filtering problem is nonlinear. Therefore the filtering technique should be capable of handling nonlinearity in the process. Hence we use the EKB filter for both linear and nonlinear delay differential equations. In order to present the equations for propagation of the estimate and error covariance, we express Eq.(61) in the non-delayed form of the nonlinear optimal filtering problem described in Eq.(57). Assuming the augmented delayed state to be incorporated in a finite-dimensional state $\mathbf{X}$, i.e., $\mathbf{X}^T(t) = [\mathbf{Y}^T(t),\ \mathbf{a}^T(t)]$, equation (61) can be written as a nonlinear optimal filtering problem without delay in the Itô form

$$\begin{aligned} d\mathbf{X}(t) &= \boldsymbol{\mathcal{F}}(\mathbf{X}, t)dt + \boldsymbol{\mathcal{G}}(t)d\boldsymbol{\beta}(t), \\ d\mathbf{z} &= \boldsymbol{\mathcal{H}}(\mathbf{X}, t)dt + \mathbf{J}(t)d\boldsymbol{\eta}(t). \end{aligned} \tag{62}$$

In order to use the EKB filter, a linearization of both $\boldsymbol{\mathcal{F}}(\cdot)$ and $\boldsymbol{\mathcal{H}}(\cdot)$ is needed. Rather than linearizing about a reference trajectory, the EKB filter employs a linearization about the state estimate itself. We also note that the time delay may be estimated similar to any parameter. For this purpose, however, it turns out to be far easier to estimate the delay by first normalizing the time via $t = \tau t'$ (which brings τ out as a coefficient in the $\mathbf{A}_1$ and $\mathbf{A}_2$ matrices and nonlinear function $\mathbf{g}(\cdot)$) before employing CSCTA, rather than estimating τ directly from Eq.(61).

To this end, we utilize the following structure for a nonlinear observer which, as in the case of the conventional KB filter, is obtained by taking the expectation of the dynamic model and adding a feedback term consisting of the measurement residual times an (as yet) unknown gain matrix, i.e.,

$$d\hat{\mathbf{X}}(t) = E[\boldsymbol{\mathcal{F}}(\mathbf{X}, t)]dt + \mathbf{L}(t)[d\mathbf{z}(t) - E[\boldsymbol{\mathcal{H}}(\mathbf{X}, t)]dt] \tag{63}$$

where $\hat{\mathbf{X}} = E[\mathbf{X}]$ denotes the estimated state. The differential observation error is

$$\begin{aligned} d\mathbf{e}(t) &= d\mathbf{X}(t) - d\hat{\mathbf{X}}(t) \\ &= \boldsymbol{\mathcal{F}}(\mathbf{X},t)dt - E[\boldsymbol{\mathcal{F}}(\mathbf{X},t)]dt - \mathbf{L}(t)\left(\boldsymbol{\mathcal{H}}(\mathbf{X},t)dt - E[\boldsymbol{\mathcal{H}}(\mathbf{X},t)]dt\right) + d\boldsymbol{B}(t) \end{aligned} \quad (64)$$

where $d\boldsymbol{B}(t) = \boldsymbol{\mathcal{G}}(t)d\boldsymbol{\beta}(t) - \mathbf{L}(t)\mathbf{J}(t)d\boldsymbol{\eta}(t)$ is a differential Brownian motion process with

$$E[d\boldsymbol{B}(t)d\boldsymbol{B}^T(t)] = \left[\boldsymbol{\mathcal{G}}(t)\mathbf{Q}\boldsymbol{\mathcal{G}}^T(t) + \mathbf{L}(t)\mathbf{J}(t)\mathbf{R}\mathbf{J}^T(t)\mathbf{L}^T(t)\right]dt. \quad (65)$$

Linearizing about the current estimate yields

$$\begin{aligned} \boldsymbol{\mathcal{F}}(\mathbf{X},t) &= \boldsymbol{\mathcal{F}}(\hat{\mathbf{X}},t) + \left.\frac{\partial \boldsymbol{\mathcal{F}}}{\partial \mathbf{X}}\right|_{\mathbf{X}=\hat{\mathbf{X}}}(\mathbf{X}-\hat{\mathbf{X}}) + \cdots, \\ \boldsymbol{\mathcal{H}}(\mathbf{X},t) &= \boldsymbol{\mathcal{H}}(\hat{\mathbf{X}},t) + \left.\frac{\partial \boldsymbol{\mathcal{H}}}{\partial \mathbf{X}}\right|_{\mathbf{X}=\hat{\mathbf{X}}}(\mathbf{X}-\hat{\mathbf{X}}) + \cdots \end{aligned} \quad (66)$$

from which $E[\boldsymbol{\mathcal{F}}(\mathbf{X},t)] = \boldsymbol{\mathcal{F}}(\hat{\mathbf{X}},t) + \cdots$ and $E[\boldsymbol{\mathcal{H}}(\mathbf{X},t)] = \boldsymbol{\mathcal{H}}(\hat{\mathbf{X}},t) + \cdots$. Truncating the Taylor series after the first order terms yields the differential observation error as

$$d\mathbf{e}(t) = [\tilde{\mathbf{F}}(t) - \mathbf{L}(t)\tilde{\mathbf{H}}(t)]\mathbf{e}(t)dt + d\mathbf{B}(t) \quad (67)$$

where $\tilde{\mathbf{F}}(t)$ and $\tilde{\mathbf{H}}(t)$ are the Jacobian matrices

$$\tilde{\mathbf{F}}(t) := \left.\frac{\partial \boldsymbol{\mathcal{F}}(\mathbf{X},t)}{\partial \mathbf{X}}\right|_{\mathbf{X}=\hat{\mathbf{X}}}, \qquad \tilde{\mathbf{H}}(t) := \left.\frac{\partial \boldsymbol{\mathcal{H}}(\mathbf{X},t)}{\partial \mathbf{X}}\right|_{\mathbf{X}=\hat{\mathbf{X}}}. \quad (68)$$

Similarly, the error covariance matrix can be obtained by differentiating $E[\mathbf{e}(t)\mathbf{e}^T(t)]$ using the Itô differential rule[94,95] to obtain

$$\begin{aligned} d\mathbf{P}(t) &= [\tilde{\mathbf{F}}(t) - \mathbf{L}(t)\tilde{\mathbf{H}}(t)]\mathbf{P}(t)dt + \mathbf{P}(t)[\tilde{\mathbf{F}}(t) - \mathbf{L}(t)\tilde{\mathbf{H}}(t)]^T dt \\ &\quad + \boldsymbol{\mathcal{G}}(t)\mathbf{Q}\boldsymbol{\mathcal{G}}^T(t)dt + \mathbf{L}(t)\mathbf{J}(t)\mathbf{R}\mathbf{J}^T(t)\mathbf{L}^T(t)dt. \end{aligned} \quad (69)$$

The optimal gain matrix $\mathbf{L}(t)$ which leads to a *minimum variance estimator* can be obtained by minimizing $\mathrm{tr}(d\mathbf{P}(t))$ which yields

$$\mathbf{L}(t) = \mathbf{P}(t)\tilde{\mathbf{H}}^T(t)\left(\mathbf{J}(t)\mathbf{R}\mathbf{J}^T(t)\right)^{-1}. \quad (70)$$

The optimal estimator so obtained is given by

$$d\hat{\mathbf{X}}(\mathbf{t}) = \boldsymbol{\mathcal{F}}(\hat{\mathbf{X}},t)dt + \mathbf{L}(t)[d\mathbf{z} - \boldsymbol{\mathcal{H}}(\hat{\mathbf{X}},t)dt] \quad (71)$$

where the covariance is propagated via the Riccati equation

$$d\mathbf{P}(t) = [\tilde{\mathbf{F}}(t)\mathbf{P}(t) + \mathbf{P}(t)\tilde{\mathbf{F}}^T(t) - \mathbf{L}(t)\tilde{\mathbf{H}}(t)\mathbf{P}(t) + \boldsymbol{\mathcal{G}}(t)\mathbf{Q}\boldsymbol{\mathcal{G}}^T(t)]dt. \quad (72)$$

We point out that the above technique is similar in concept (in that it uses CSCTA but not RLFT) to the second of the three strategies for control described in Section 3.1, i.e., by direct numerical solution of the time-dependent Riccati equation from which the control gain was obtained. In fact, the LQR and KBF problems are dual to each other. Other estimation strategies which are dual to the first and third

control strategies are also possible to formulate, in which observer design problems may also be solved by traditional pole placement without taking into account the stochastic noise in the process and measurement. In fact, such observer designs and observer-based controllers for linear and nonlinear periodic systems of ODEs which utilize the Liapunov-Floquet transformation were proposed in Refs.87, 96, respectively. Hence, we point out that observer designs for periodic DDEs dual to the controller formulation based on CSCTA, RLFT, and the auxiliary systems in Section 4.1 are possible. However, we do not explore this concept further here since the KBF-based estimator will be used in the following example as well as in the observer-based feedback control design for attitude control in Section 6.

5.2. *Parametrically Forced Second Order Nonlinear DDE*

Consider a second order damped delayed system with cubic nonlinearity and a parametric sinusoidal excitation as

$$\ddot{x}(t) + kx(t) + \epsilon x^3(t) + c\dot{x}(t) = f_1 x(t-1) + f_2 \sin(2\pi t)x(t) + v(t) \tag{73}$$

where the the position $x(t)$ and velocity $\dot{x}(t)$ are measured directly and the parameter vector of the system is $\mathbf{a} = [k, f_2, c, f_1, \epsilon]$ with a true value of $\mathbf{a} = [7, 5, 0.05, 0.1, 1]$. After performing a convergence study the delay system is approximated with a set of ODEs using 8 Chebyshev collocation points.

First, the states and all five parameters of the system are simultaneously estimated from a noise-corrupted measurement. The above DDE is integrated using the `dde23` function in Matlab[97] with a time step of $dt = 0.0001$ sec. The response corrupted by an additive zero-mean Gaussian noise $\mathbf{w}(t)$ with a covariance of $\mathbf{R} = 0.1\mathbf{I}$ is fed into the filtering algorithm with a measurement function of $\mathbf{h}(\mathbf{Y}(t)) = \mathbf{Y}_1(t)$ as the continuous-time measured states. The estimation filtering sequence is initiated with a first guess for the unknown parameters as $\mathbf{a}_0 = [5, 3, 0.5, 0.8, 2]$. In order to account for uncertainties in the acceleration model a zero-mean Gaussian noise $v(t)$ with a variance of $Q = 0.1$ is included in the process state. The initial value of the error covariance matrix $\mathbf{P}_0$ is $10\mathbf{I}$. Note that the augmented state-space process of the Eq.(61) is comprised of 2 primary states (the second of which includes the process noise) plus 16 discretized delayed states plus 5 augmented parameter states. The results of using EKB filter for simultaneous estimation of the states and the unknown parameters are shown in Fig.11. The estimated unknown parameters are $\hat{\mathbf{a}} = [6.963, 4.984, 0.056, 0.107, 1.006]$ with an average error of 4.38%.

The quality of the measurements represented by the stochastic term $\mathbf{w}(t)$ and the extent of uncertainty of the model represented by stochastic term $v(t)$, are two determining factors in the accuracy of the estimated parameters using the current approach. To show this, we reduce the variance of process and covariance of measurement noise to $Q = 10^{-4}$ and $\mathbf{R} = 10^{-4}\mathbf{I}$. The initial value of the error covariance matrix is also reduced relatively to $\mathbf{P}_0 = 0.1\mathbf{I}$ while the initial guess for the unknown parameters $\mathbf{a}_0$ is still the same. Following the same approach

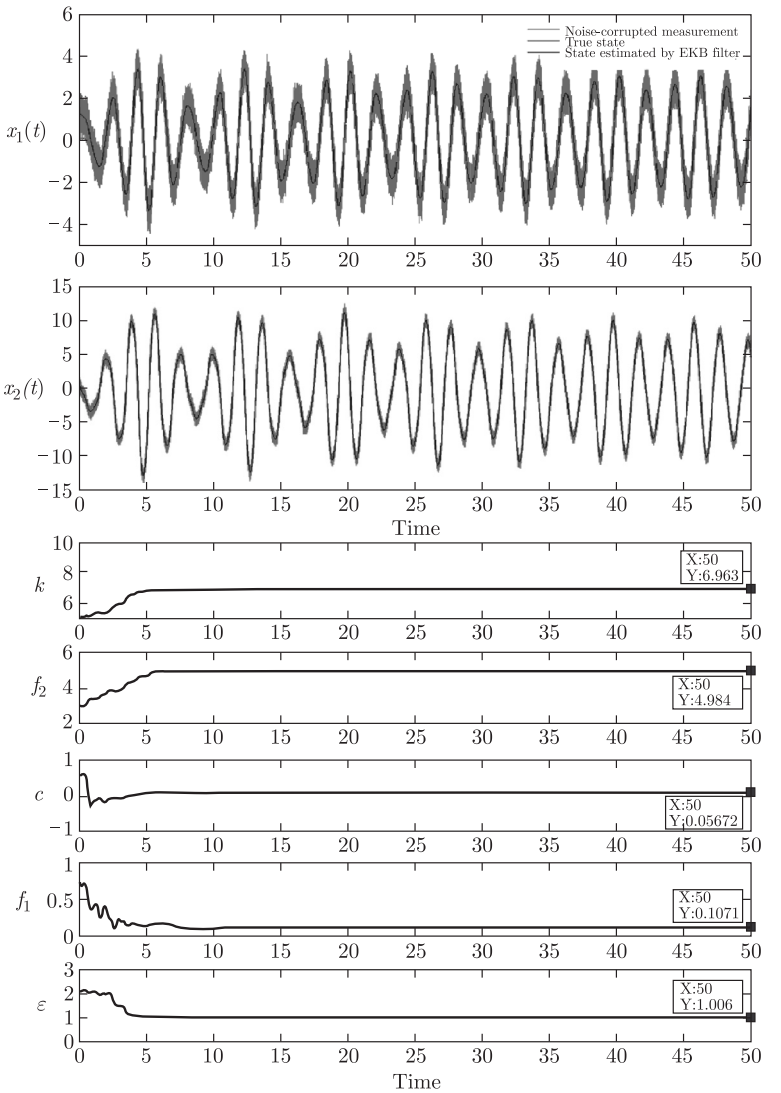

Fig. 11. States and parameters of the parametrically forced second order nonlinear DDE of Eq.(73) estimated from noise-corrupted measurement using EKB filter.

using CSCTA and the EKB filter yields the estimated vector of unknowns with an improved accuracy as $\hat{\mathbf{a}} = [6.99, 5.00, 0.05, 0.10, 1.00]$ which has only 0.02% error on average.

So far, the state observation has been assumed to be complete, i.e., there exist measurements of all state components of the system, and the time delay has been assumed to be known exactly. However in some real-world situations it frequently happens that one or more of the states cannot be measured and the time delay is not known. However, the EKB filter can still be used for estimation in case of

an incomplete measurement as long as the system remains observable. In fact, the EKB filter can be used to estimate a globally-observable process by sequentially incorporating only measurements of locally unobservable processes provided that sufficient number of measurements is taken[98]. Also, the time delay may be treated as a parameter multiplying the $\mathbf{A}_1$ and $\mathbf{A}_2$ matrices and vector $\mathbf{g}(\cdot)$ in Eqs.(58) and (59) by a transformation $t = \tau t'$ to a nondimensional time t' in which the delay is normalized to unity, after which state augmentation and CSCTA may be applied as before. In this way, the time delay itself is estimated just as the parameters are estimated in Fig.11.

The nonlinear DDE of Eq.(73) is now reconsidered where only the position $x(t)$ is measured, i.e., it is assumed that the velocity $\dot{x}(t)$ is unobserved and no measurement is available from this state. In addition, the initial guess $\hat{\tau}_0 = 3$ for the unknown time delay is twice the true value ($\tau = 1.5$), and the remaining five parameters are now fixed to the same true values as before (i.e., they are not estimated). The covariances of the measurement and process noise are reduced to $\mathbf{R} = \mathbf{Q} = 0.1\mathbf{I}$. The filtering sequence is initiated with the same initial value of the error covariance matrix. The estimated time delay along with the observed and unobserved states of the system estimated using EKB filter are depicted in Fig.12.

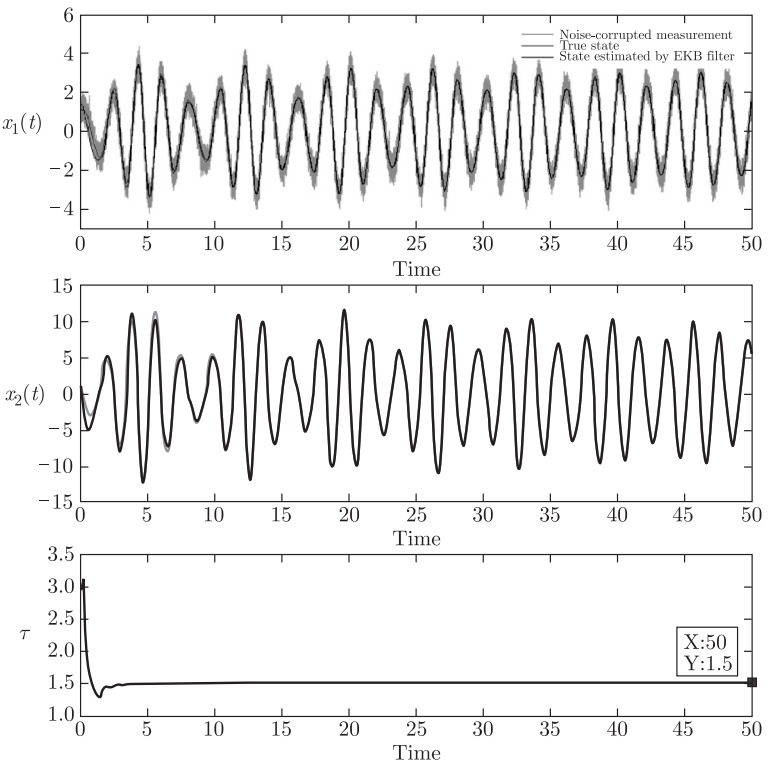

Fig. 12. States and estimated delay of the parametrically forced second order nonlinear DDE of Eq.(73) with unknown time delay estimated from noise-corrupted measurement of $x(t)$ and without any measurement of $\dot{x}(t)$ using EKB filter.

The estimate of the time delay converges to its true value in under 10 sec while the estimated states show a good accuracy. Note that the state $x_2(t) = \dot{x}(t)$ is estimated with absolutely no measurement of this state.

6. Application to Observer-based Delayed Feedback Control of Spacecraft Attitude

The observer-based attitude control of a rigid spacecraft with nonlinear delayed multi-actuator feedback control is studied in this section. It is assumed that the time delay occurs in one of the actuators (e.g., reaction control thruster) while the other actuator (e.g., reaction wheel (RW) or control moment gyro (CMG)) does not have significant time delay. This is relevant to the problem of spacecraft desaturation maneuvers in which the RW or CMG is brought to its null state while using the thruster to keep the spacecraft motionless without a resulting torque applied. Figure 13 shows the block diagram of the system with time delay in one of the actuators, where actuator 1 is nondelayed with gains k_1 and k_2, while actuator 2 has time delay with gain k_3. Therefore, a nonlinear feedback controller using both delayed and nondelayed states is sought for the controlled system to have the desired linear delayed closed-loop dynamics using an inverse dynamics approach. The attitude modeling problem depends on the choice of attitude parameters to represent the orientation of a rigid body relative to an inertial frame. There are several different attitude parametrizations which can be utilized. Here, we utilize the modified Rodriguez parameters (MRPs), which are a minimal three-parameter set defined as a stereographic projection of the Euler parameters (quaternions). Furthermore, if switching to the shadow set is employed when the principal angle passes through 180 deg, then the MRPs are unique and singularity-free[99].

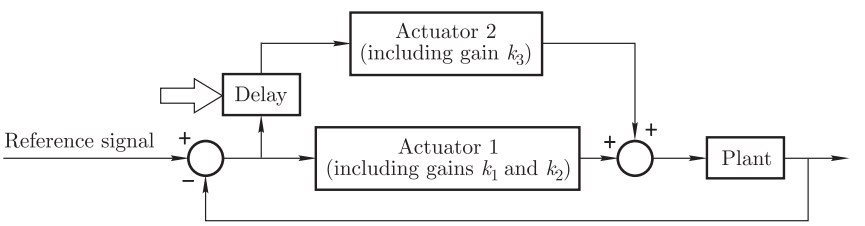

Fig. 13. The block diagram of the system with the time delay in one of the actuators

Consider the attitude dynamics of a rigid spacecraft as

$$\begin{aligned} \dot{\boldsymbol{\sigma}}(t) &= \frac{1}{4}\mathbf{B}(\boldsymbol{\sigma}(t))\boldsymbol{\omega}(t), \\ \dot{\boldsymbol{\omega}}(t) &= -\mathbf{J}^{-1}\boldsymbol{\omega}^{\times}(t)\mathbf{J}\boldsymbol{\omega}(t) + \mathbf{J}^{-1}\mathbf{u}(t) \end{aligned} \tag{74}$$

where $\boldsymbol{\omega} \in \mathbb{R}^3$ represents the body-frame angular velocity vector, $\boldsymbol{\sigma}(t) \in \mathbb{R}^3$ is the MRP set, $\mathbf{u}(t) \in \mathbb{R}^3$ is the control input, $\mathbf{J}$ is the 3×3 symmetric inertia matrix,

and

$$\mathbf{B}(\boldsymbol{\sigma}) = \left[(1 - \boldsymbol{\sigma}^T\boldsymbol{\sigma})\mathbf{I}_{3\times 3} + 2\boldsymbol{\sigma}^{\times} + 2\boldsymbol{\sigma}\boldsymbol{\sigma}^T\right]. \tag{75}$$

Note that $(\cdot)^{\times} : \mathbb{R}^3 \to \mathrm{so}(3)$ is the skew-symmetric mapping given by

$$\boldsymbol{\Gamma}^{\times} = \begin{bmatrix} 0 & -\Gamma_3 & \Gamma_2 \\ \Gamma_3 & 0 & -\Gamma_1 \\ -\Gamma_2 & \Gamma_1 & 0 \end{bmatrix} \tag{76}$$

where the space of 3×3 real skew-symmetric matrices is denoted by so(3), the Lie algebra of the Lie group SO(3).

6.1. *Inverse Dynamics Approach for Feedback Control Law*

There are different approaches for controlling the attitude dynamics of a rigid body. One method is to assume a linear control law which results in a nonlinear model for the closed-loop dynamics of the system[36,41]. Another method is to assume a nonlinear control law which results in a linear model for the closed-loop dynamics of the system[99]. The second approach will be utilized in this section. In particular, an inverse dynamics approach common in robotics open-loop path-planning problems is utilized here, in which the desired closed-loop response is approximated by a set of second order delay differential equations. This approach (without time delay) has been used in the attitude control problem using both MRPs[99] and quaternions[100].

Based on the desired closed-loop dynamics for the delay-free case[99], for the delayed system, we assume that the desired closed-loop system is

$$\ddot{\boldsymbol{\sigma}}(t) + k_1\dot{\boldsymbol{\sigma}}(t) + k_2\boldsymbol{\sigma}(t) = k_3\boldsymbol{\sigma}(t-\tau) \tag{77}$$

where k_1, k_2, and k_3 are scalar control gains. The body angular acceleration vector corresponding to Eq.(77) can be simplified to[40]

$$\begin{aligned}\dot{\boldsymbol{\omega}}(t) = -k_1\boldsymbol{\omega}(t) - \left[\boldsymbol{\omega}(t)\boldsymbol{\omega}^T(t) + \left(\frac{4k_2}{1+||\boldsymbol{\sigma}(t)||^2} - \frac{||\boldsymbol{\omega}(t)||^2}{2}\right)\mathbf{I}_{3\times 3}\right]\boldsymbol{\sigma}(t) \\ +4\mathbf{B}^{-1}(\boldsymbol{\sigma}(t))k_3\boldsymbol{\sigma}(t-\tau).\end{aligned} \tag{78}$$

By following the inverse dynamics approach[40], it can be shown that the nonlinear control law given by

$$\begin{aligned}\mathbf{u}(t) = \boldsymbol{\omega}^{\times}(t)\mathbf{J}\boldsymbol{\omega}(t) - \mathbf{J}k_1\boldsymbol{\omega}(t) \\ -\mathbf{J}\left[\boldsymbol{\omega}(t)\boldsymbol{\omega}(t)^T + \left(\frac{4k_2}{1+||\boldsymbol{\sigma}(t)||^2} - \frac{||\boldsymbol{\omega}(t)||^2}{2}\right)\mathbf{I}_{3\times 3}\right]\boldsymbol{\sigma}(t) \\ +4\mathbf{J}\frac{1}{\left[1+||\boldsymbol{\sigma}(t-\tau)||^2\right]^2}\mathbf{B}^T(\boldsymbol{\sigma}(t-\tau))k_3\boldsymbol{\sigma}(t-\tau)\end{aligned} \tag{79}$$

can locally asymptotically stabilize the system in Eq.(74) if the scalar control gains k_1, k_2, and k_3 are selected such that equation (77) is stable. Hence, the closed-loop stability is given by the same second-order DDE for which the Hsu-Bhatt-Vyshnegradskii stability chart can be used to select stable control gains. In the controller given in Eq.(79), the first three nondelayed terms correspond to the control force in actuator 1 in Fig.13, while the last term depending on the delayed MRP parameter set corresponds to the control force in actuator 2.

6.2. *Observer-based Controller Design*

6.2.1. *Delayed Feedback Control from Estimated States*

In developing the feedback control law in Section 6.1, both the MRP parametrization $\boldsymbol{\sigma}(t)$ and the angular velocity $\boldsymbol{\omega}(t)$ of the rigid body are assumed to be available. A problem arises if the internal states of the system are not known, in which case we can design an observer or estimator that attempts to reconstruct the internal state vector of the plant using measurable noisy outputs in a way that is applicable in state feedback. Assuming the system is controllable and observable, the controlled model with measurements takes the form of

$$\begin{bmatrix}\dot{\boldsymbol{\sigma}}(t)\\ \dot{\boldsymbol{\omega}}(t)\end{bmatrix}=\begin{bmatrix}\frac{1}{4}\mathbf{B}(\boldsymbol{\sigma}(t))\boldsymbol{\omega}(t)\\ -\mathbf{J}^{-1}\boldsymbol{\omega}^{\times}(t)\mathbf{J}\boldsymbol{\omega}^{\times}(t)+\mathbf{J}^{-1}\hat{\mathbf{u}}(t)\end{bmatrix}=\mathbf{f}\left(\begin{bmatrix}\boldsymbol{\sigma}(t)\\ \boldsymbol{\omega}(t)\end{bmatrix}\right)+\mathbf{b}\hat{\mathbf{u}}(t)+\begin{bmatrix}0\\0\\0\\1\\1\\1\end{bmatrix}v(t),$$

$$\mathbf{y}=\mathbf{h}\left(\begin{bmatrix}\boldsymbol{\sigma}(t)\\ \boldsymbol{\omega}(t)\end{bmatrix},t\right)+\mathbf{w}(t) \tag{80}$$

where $v(t)$ and $\mathbf{w}(t)$ are zero-mean Gaussian noise processes, $\mathbf{b}=[\mathbf{0}_{3\times3},\ \mathbf{J}^{-1}]^T$, and $\hat{\mathbf{u}}(t)$ is the control law given by Eq.(79) wherein the states $\boldsymbol{\sigma}(t)$, $\boldsymbol{\omega}(t)$, and the delayed MRP set $\boldsymbol{\sigma}(t-\tau)$ are replaced with their estimates $\hat{\boldsymbol{\sigma}}(t),\hat{\boldsymbol{\omega}}(t),\hat{\boldsymbol{\sigma}}(t-\tau)$ obtained from the state observer. Note that the process noise is added only to the dynamics, not the kinematics.

Following Section 5.1 we employ CSCTA and define the expanded $(6(N+1)\times1)$ vector $\mathbf{Y}(t)$ as

$$\mathbf{Y}(t)=\left[\begin{bmatrix}\boldsymbol{\sigma}(t)\\ \boldsymbol{\omega}(t)\end{bmatrix}^T,\begin{bmatrix}\boldsymbol{\sigma}(t-\tau_1)\\ \boldsymbol{\omega}(t-\tau_1)\end{bmatrix}^T,\begin{bmatrix}\boldsymbol{\sigma}(t-\tau_2)\\ \boldsymbol{\omega}(t-\tau_2)\end{bmatrix}^T,\ldots,\begin{bmatrix}\boldsymbol{\sigma}(t-\tau)\\ \boldsymbol{\omega}(t-\tau)\end{bmatrix}^T\right]^T \tag{81}$$

such that $\tau_i = \frac{\tau}{2}\left(1 - \cos\frac{i\pi}{N}\right)$, $i = 1, 2, \ldots, N$, where N is the number of collocation intervals. Then, as in Section 5 the observer is given by the set of ODEs:

$$\begin{aligned}\dot{\hat{\mathbf{Y}}}(t) = &\begin{bmatrix} \mathbf{0}_{6\times6} & \mathbf{0}_{6\times6} & \cdots & \mathbf{0}_{6\times6} & \mathbf{0}_{6\times6} \\ & & \frac{2}{\tau}\mathbb{D}^{(7:6(N+1),:)} & & \end{bmatrix}\hat{\mathbf{Y}}(t) \\ &+ \begin{bmatrix} \mathbf{f}\left(\hat{\mathbf{Y}}_1(t)\right) \\ \mathbf{0}_{6N\times1} \end{bmatrix} + \begin{bmatrix} \mathbf{b} \\ \mathbf{0}_{6N\times3} \end{bmatrix}\hat{\mathbf{u}}(t) + \mathbf{L}(t)\left[\mathbf{y}(t) - \mathbf{h}\left(\hat{\mathbf{Y}}_1(t), t\right)\right] \\ = &\ \boldsymbol{\mathcal{F}}\left(\hat{\mathbf{Y}}(t)\right) + \boldsymbol{\mathcal{B}}\hat{\mathbf{u}}(t) + \mathbf{L}(t)\left[\mathbf{y}(t) - \mathbf{h}\left(\hat{\mathbf{Y}}_1(t), t\right)\right] \end{aligned} \tag{82}$$

where the differential operator $\mathbb{D}$ can be obtained as described in Section 2.1. The observer above delivers the estimated states $\hat{\boldsymbol{\omega}}(t)$, $\hat{\boldsymbol{\sigma}}(t)$, and $\hat{\boldsymbol{\sigma}}(t-\tau)$ which are required to form the control input $\hat{\mathbf{u}}(t)$ in Eq.(80). Therefore, the observer-based controller using the KBF as in Section 5 can be expressed as

$$\begin{aligned}\dot{\mathbf{Y}}(t) = &\ \boldsymbol{\mathcal{F}}(\mathbf{Y}(t)) + \boldsymbol{\mathcal{B}}\hat{\mathbf{u}}(t) + \boldsymbol{\mathcal{G}}v(t), \\ \mathbf{y}(t) = &\ \mathbf{h}\left(\mathbf{Y}_1(t), t\right) + \mathbf{w}(t), \\ \dot{\hat{\mathbf{Y}}}(t) = &\ \boldsymbol{\mathcal{F}}\left(\hat{\mathbf{Y}}(t)\right) + \boldsymbol{\mathcal{B}}\hat{\mathbf{u}}(t) + \mathbf{L}(t)\left[\mathbf{y}(t) - \mathbf{h}\left(\hat{\mathbf{Y}}_1, t\right)\right], \\ \hat{\mathbf{u}}(t) = &\ \hat{\boldsymbol{\omega}}^{\times}(t)\mathbf{J}\hat{\boldsymbol{\omega}}(t) - \mathbf{J}k_1\hat{\boldsymbol{\omega}}(t) \\ &- \mathbf{J}\left[\hat{\boldsymbol{\omega}}(t)\hat{\boldsymbol{\omega}}(t)^T + \left(\frac{4k_2}{1+||\hat{\boldsymbol{\sigma}}(t)||^2} - \frac{||\hat{\boldsymbol{\omega}}(t)||^2}{2}\right)\mathbf{I}_{3\times3}\right]\hat{\boldsymbol{\sigma}}(t) \\ &+ 4\mathbf{J}\frac{1}{\left[1+||\hat{\boldsymbol{\sigma}}(t-\tau)||^2\right]^2}\mathbf{B}^T(\hat{\boldsymbol{\sigma}}(t-\tau))k_3\hat{\boldsymbol{\sigma}}(t-\tau) \end{aligned} \tag{83}$$

where $\boldsymbol{\mathcal{G}} = [0,\ 0,\ 0,\ 1,\ 1,\ 1,\ 0,\ \ldots,\ 0]^T$, and the KBF observer gain is $\mathbf{L}(t) = \mathbf{P}(t)\tilde{\mathbf{H}}^T(t)\mathbf{R}^{-1}$ where $\mathbf{R}$ is the covariance of the measurement noise. $\mathbf{P}(t)$ is the error covariance propagated with Eq.(83) as

$$\dot{\mathbf{P}}(t) = \tilde{\mathbf{F}}(t)\mathbf{P}(t) + \mathbf{P}(t)\tilde{\mathbf{F}}^T(t) - \mathbf{L}(t)\tilde{\mathbf{H}}(t)\mathbf{P}(t) + \boldsymbol{\mathcal{G}}(t)\mathbf{Q}\boldsymbol{\mathcal{G}}^T(t) \tag{84}$$

where $\tilde{\mathbf{H}}(t)$ and $\tilde{\mathbf{F}}(t)$ are the Jacobians in Eq.(68).

6.2.2. *Delayed Feedback Control from Estimated Delay and State*

As mentioned in the previous section, if parameters of the system are not known the observer can be designed to estimate the parameters along with the states in a way that is applicable in the state feedback. The control law of Eq.(79) requires

the current states $\boldsymbol{\sigma}(t)$ and $\boldsymbol{\omega}(t)$ and the delayed MRP set $\boldsymbol{\sigma}(t-\tau)$. Since the approach used for designing the observer in the observer-based controller was shown in Section 5 to be also capable of estimating the delay, another observer can be designed to generate estimates of the current states $\hat{\boldsymbol{\sigma}}(t)$, $\hat{\boldsymbol{\omega}}(t)$, and the time delay $\hat{\tau}$. Therefore, the estimated delayed MRP set can be obtained by first finding the estimated current states and then moving back in time to the extent of the estimated delay. Obviously, the observer error in this case is expected to be more than in the case where both the current and the delayed states are directly estimated and the fixed time delay is assumed to be known.

6.3. *Simulation Results*

Numerical simulations of the observer-based controllers described in Sections 6.2.1 and 6.2.2 are discussed in this section. In the first simulation the observer estimates the current states and the delayed MRP. The combined observer-controller of Eq.(83) is applied with an inertia matrix of $\mathbf{J} = \text{diag}([30, 20, 10])$ kg $\cdot$ m^2. The measurement function is assumed to be $\mathbf{h}(\mathbf{Y}_1) = \mathbf{Y}_1$ and corrupted with a zero-mean Gaussian noise of the covariance $\mathbf{R} = 1 \times 10^{-4}\mathbf{I}$. The initial state of the system is assumed to be $[\boldsymbol{\sigma}_0^T,\ \boldsymbol{\omega}_0^T]^T = [-0.3, -0.4, 0.2, 0.2, 0.2, 0.2]^T$ and no process noise is assumed to exist ($\mathbf{Q} = \mathbf{0}$). The error covariance propagation is initialized with $\mathbf{P}_0 = 1 \times 10^{-2}\mathbf{I}$ and the initial guess for the estimated states of the system is assumed to be 50% deviated from the true state. The controller parameters are $k_1 = 8$, $k_2 = 16$, $k_3 = 8$, the time delay is assumed to be $\tau = 0.5$ sec, and 10 Chebyshev collocation points are used in CSCTA. The combined observer-controller states are compared with those of the controller without any observer in Fig.14, in which it is seen that the combined delayed state feedback controller/observer successfully brings the states of the rigid spacecraft to zero.

In the second simulation the observer estimates only the current states and the delay. The delayed MRP is obtained by moving back in time to the extent of the estimated delay. The measurement function is assumed to be the same as before but corrupted with a zero-mean Gaussian noise of the covariance $\mathbf{R} = 1 \times 10^{-5}\mathbf{I}$. The initial state of the system is again $[\boldsymbol{\sigma}_0^T,\ \boldsymbol{\omega}_0^T]^T = [-0.3, -0.4, 0.2, 0.2, 0.2, 0.2]^T$ and the process noise has a variance of $Q = 1 \times 10^{-5}$. The error covariance propagation is initialized with $\mathbf{P}_0 = 1 \times 10^{-3}\mathbf{I}$ and the initial guess for the estimated states of the system is assumed to be 50% deviated from the true state. The controller parameters are $k_1 = 8$, $k_2 = 16$, $k_3 = 8$, the true value of the time delay is assumed to be $\tau = 0.95$ sec, and 10 Chebyshev collocation points are used in CSCTA. The estimated delay is depicted in Fig.15 as well as the comparison between the observer-based controlled states and those of the controller without any observer (assuming the true states are available for feedback). As clear from the figure, the estimated delay converges to the close vicinity of the true delay after 2 seconds. As expected, the estimation error in this case is more than in the case where the delayed states are directly estimated with the constant time delay assumed to be known.

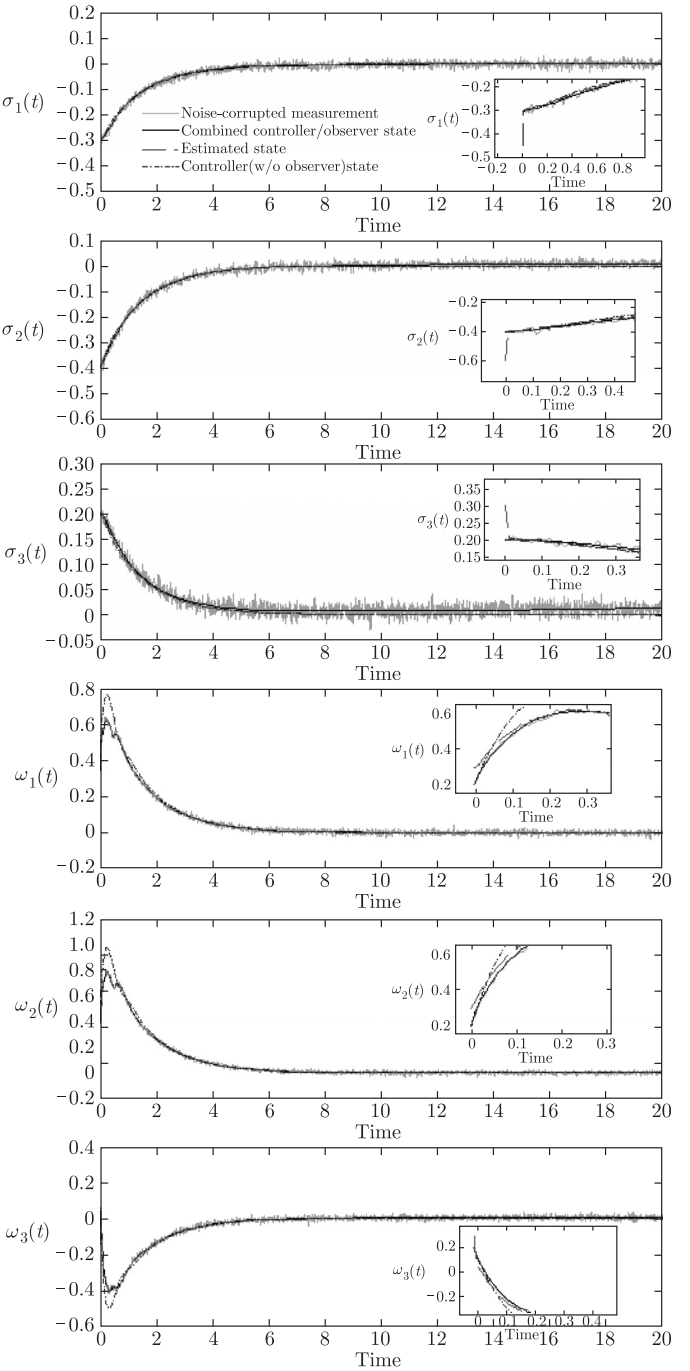

Fig. 14. The estimated attitude states $\boldsymbol{\sigma}$, and angular velocity components $\boldsymbol{\omega}$ of the controller without observer compared with those of the observer-based controller where the delayed states are directly estimated and the fixed time delay is assumed to be known.

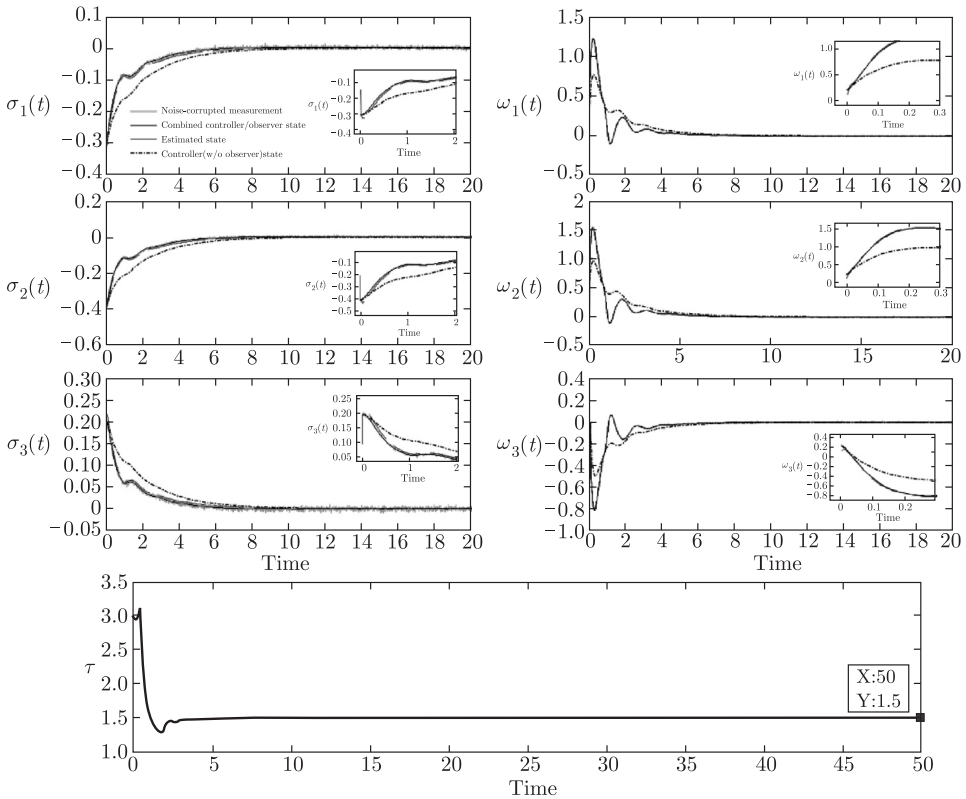

Fig. 15. The estimated attitude states $\boldsymbol{\sigma}$, angular velocity components $\boldsymbol{\omega}$, and time delay τ of the controller without observer compared with those of the observer-based controller where the delayed states are estimated using the estimated delay.

7. Conclusions

In this chapter, the authors have presented two different numerical approaches, based on the Chebyshev spectral continuous time approximation and reduced Liapunov-Floquet transformation, respectively, for estimation and control of (retarded) linear and nonlinear time-delayed systems with discrete or distributed delay and (possibly) time-periodic coefficients. The CSCTA method, which effectively removes the time delay by converting the (possibly nonlinear) DDEs into an approximate large-dimensional set of ODEs, is applicable to both time-invariant and time-varying systems. This method uses Chebyshev collocation and the spectral differentiation operational matrix associated with the unequally-spaced Chebyshev collocation points. The main advantage of this strategy (as opposed to finite differences, for instance) is in its spectrally accurate exponential convergence characteristics. The RLFT technique, which effectively removes the time-periodic coefficients of the resulting time-periodic linear ODEs after applying CSCTA to a system of

time-periodic linear DDEs, is specifically used in conjunction with CSCTA for periodic delayed systems. Thus, the resulting low-dimensional set of constant-coefficient ODEs (i.e., Eq.(29)) exactly preserves the eigenstructure (including the dominant characteristic exponents) of the delayed system as represented in the transformed domain (i.e., Eq.(23)). Approximate expressions for the RLFT matrix (i.e., Eqs.(32) and (33)) and its inverse (obtained from the adjoint system) were provided. For linear control problems with delayed feedback or nonlinear delayed systems with a non-vanishing linear part, the combination of CSCTA and RLFT results in a low-dimensional system with time-invariant linear part and periodic coefficients multiplying the control or nonlinear term. Several illustrative examples were used to demonstrate the techniques, including a scalar time-invariant DDE (in which the CSCTA form was compared with the continuous time approximation obtained using forward and centered finite differences) and various forms of the delayed Mathieu equation with single and multiple discrete delays as well as discontinuous distributed delay. It should be noted that no discussion of delay or parametric resonances and their effects on the RLFT were provided, but the reader is directed to Ref.53 for further discussion of this issue.

Next, the control problem associated with time-invariant and time-periodic delayed systems was discussed, in which three strategies were suggested for designing closed-loop feedback controllers. It is shown that using the CSCTA and RLFT methods can help to reduce a (possibly time-periodic) nonlinear delayed system with linear and/or nonlinear feedback control into a form more conducive for the application of many techniques for control of delayed and non-delayed systems in the literature. Specifically, the following three strategies were suggested for designing closed-loop linear feedback controllers for linear periodic delayed systems. First, the stability of the closed-loop response may be investigated in the parameter space of available control gains using Floquet theory, and the optimal control gains may be found for a minimum spectral radius. This strategy does not use either CSCTA or RLFT but instead utilizes one of several existing techniques (e.g., Chebyshev collocation, semi-discretization, and temporal finite elements) to construct a linear map representation (which approximates the monodromy operator) of the closed-loop periodic DDE system. An example of a controlled delayed Mathieu equation illustrated this strategy in which the periodic control gains utilized a three-term Fourier series with coefficients to be obtained by sequentially selecting higher order pairs of gain coefficients that minimize the spectral radius of the closed-loop system. Second, the use of optimal control (time-varying LQR) was suggested in which a time-varying Riccati equation is solved directly from which the time-varying control gain matrix is obtained. This method utilizes CSCTA to obtain an equivalent set of ODEs for which the LQR control is designed, but does not use RLFT. Finally, the third suggested strategy involves the use of both CSCTA and RLFT as well as either pole placement or optimal control design for linear time-invariant systems. Specifically, the sequential application of both CSCTA and RLFT enables the con-

trol design to take place in a transformed coordinate system in which both the delay and periodic coefficients are effectively removed, thereby enabling the use of traditional control design tools for linear time-invariant systems. Although the stability for underactuated systems cannot be guaranteed using this approach due to use of a least squares inverse to solve for the time-periodic control gain matrix, the alternative use of a backstepping strategy for time-periodic systems[88] would guarantee asymptotic stability even for these cases. Additional linear control strategies not discussed here that could be employed in conjunction with CSCTA and RLFT include output feedback and observer-based control, while possible nonlinear control strategies to be used with CSCTA and RLFT include nonlinear reduced order controllers, bifurcation controllers, and chaos controllers. The authors are currently planning the investigation of these alternatives.

Next, the estimation of states, parameters, and delay for nonlinear delayed systems using optimal stochastic filtering from noise-corrupted, possibly incomplete measurements was explored using CSCTA. After discretizing the delayed system with a set of ordinary differential equations, the stochastic estimation problem was implemented via state augmentation (to include the unknown parameters and/or delay in the estimate) and by using an extended Kalman-Bucy filter to propagate the equations for the estimate and the state error covariance (through a time-varying Riccati equation). In contrast to the standard Kalman-Bucy filter which employs a linearization about a reference solution, in the extended version the linearization is about the estimate itself (similar to the extended Kalman filter for discrete estimation), thus providing additional accuracy for nonlinear estimation problems. An example of a second order damped system with cubic nonlinearity forced by a delayed term and parametric excitation served as an illustrative example in which two estimation scenarios were analyzed: a) The two states (position and velocity) along with five parameters were estimated from full noise-corrupted state measurements, and b) the two states and the time delay were estimated from incomplete noise-corrupted measurements of the position only. Initial errors in the states, parameters, and delay along with a process noise to help account for unmodeled dynamics were employed in each case. This optimal estimator can also be employed to provide estimated states, parameters, and delay to be used in an observer-based feedback controller. For an illustrative example in a practical engineering problem, the problem of spacecraft attitude estimation and multi-actuator regulation control in the presence of an unknown time delay in one actuator was discussed and illustrated with simulations. This problem is relevant to spacecraft desaturation maneuvers in which the reaction wheel or control moment gyro is brought to its null state while using a reaction control thruster to keep the spacecraft motionless without a resulting torque applied. A nonlinear feedback controller using both delayed and non-delayed states was employed in order for the closed-loop system to have the desired linear dynamics using an inverse dynamics approach along with modified Rodriguez parameters for the attitude parameterization. The results demonstrated

that the observer-based delayed feedback regulation controller can successfully stabilize a desired attitude in the presence of noisy measurements and unknown time delay. Future planned research efforts will include the investigation of alternative control laws obtained through the use of Liapunov-Krasovskii functionals and linear matrix inequalities, more realistic attitude measurement models, and the application of these methods to the more difficult problem of delayed feedback attitude estimation and control of dual-spin spacecraft.

Acknowledgments. The first author would like to thank colleagues Brian Mann, Hanspeter Schaub, and Amit Sanyal. The support of NSF grants CMMI-0900289 and CMMI-1131646 is gratefully appreciated.

References

1. N. Krasovskii, *Stability of Motion*: *Applications of Lyapunov's Second Method to Differential Systems and Equations with Delay* (Stanford University Press, Stanford, 1963).
2. L. Pontryagin, On the zeros of some elementary transcendental functions (in Russian), *Izvestiya Akademii Nauk SSSR.*, **6**, 115–134 (1942). (English translation in American Mathematical Society Translations, 96–110, 1955.)
3. N. Chebotarev and N. Meiman, The Routh-Hurwitz problem for polynomials and entire functions (in Russian), *Trudy Matematicheskogo Instituta imeni V. A. Steklova.*, **26**, 3–331 (1949).
4. N. Hayes, Roots of the transcendental equations associated with certain differential-difference equations, *Journal of the London Mathematical Society*, **25**, 226–232 (1950).
5. R. Bellman and K. Cooke, *Differential-Difference Equations* (Academic, 1963).
6. K. Gu, V. Kharitonov, and J. Chen, *Stability of Time-Delay Systems* (2003).
7. T. Insperger and G. Stépán, *Semi-Discretization for Time-Delay Systems*: *Stability and Engineering Applications* (Springer, New York, 2011).
8. W. Michiels and S.-I. Niculescu, *Stability and Stabilization of Time-delay Systems*: *an Eigenvalue-based Approach* (SIAM Press, Philadelphia, 2008).
9. S.-I. Niculescu, *Delay Effects on Stability. A Robust Control Approach* (Springer-Verlag, London, 2001).
10. G. Stépán, *Retarded Dynamical Systems*: *Stability and Characteristic Functions* (Longman Scientific and Technical, Harlow, UK, 1989).
11. F. Khasawneh and B. Mann, Stability of delay integro-differential equations using a spectral element method, *Mathematical and Computer Modeling*, **54**(9–10), 2493–2503 (2011).
12. O. Bobrenkov, M. Nazari, and E. Butcher, Response and stability analysis of periodic delayed systems with discontinuous distributed delay, *Journal of Computational and Nonlinear Dynamics*, **7**, (2012).
13. F. Khasawneh, B. Mann, T. Insperger, and G. Stépán, Increased stability of low-speed turning through a distributed force and continuous delay model, *Journal of Computational and Nonlinear Dynamics*, **4**(4), 1–12 (2009).
14. S. Mondie, M. Dambrine, and O. Santos, Approximation of control laws with distributed delays: a necessary condition for stability, *Kybernetika*, **38**, 541–551 (2002).

15. W. Hahn, On difference differential equations with periodic coefficients, *Journal of Mathematical Analysis and Application*, **8**, 70–101 (1961).
16. A. Stokes, A floquet theory for functional differential equations, *Proceedings of the National Academy of Sciences, USA*, **48**, 1330–1334 (1962).
17. E. Butcher and B. Mann, *Stability Analysis and Control of Linear Periodic Delayed Systems Using Chebyshev and Temporal Finite Element Methods* (*Delay Differential Equations*: *Recent Advances and New Directions*, B. Balachandran, D. Gilsinn, and T. Kalmar-Nagy (Ed.), New York (2009).
18. E. Butcher, O. Bobrenkov, E. Bueler, and P. Nindujarla, Analysis of milling stability by the Chebyshev collocation method: algorithm and optimal stable immersion levels, *Journal of Computational and Nonlinear Dynamics*, **3**, 1–12 (2009).
19. F. Khasawneh, B. Mann, and E. Butcher, A multi-interval Chebyshev collocation approach for the stability of periodic delayed systems with discontinuities, *Communications in Nonlinear Science and Numerical Simulation*, **16**, 4408–4421 (2011).
20. V. Yakubovich and V. Starzhinski, *Linear Differential Equations with Periodic Coefficients, Parts* 1–2 (Wiley, New York, 1975).
21. Y. Orlov, L. Belkoura, J. Richard, and M. Dambrine, Online parameter identification of linear time delay systems, *Proceedings of the* 41*st IEEE Conference on Decision and Control, Las Vegas, NV, USA*, **1**, 630–635 (2002).
22. M. Basin, P. Shi, and D. Calderon-Alvarez, Optimal state filtering and parameter identification for linear time-delay systems, *Proceedings of the American Control Conference, Seattle, USA*, 7–12 (2008).
23. N. Ahmedova, V. Kolmanovskii, and A. Matasov, Constructive filtering algorithms for delayed systems with uncertain statistics, *Journal of Dynamic Systems, Measurement, and Control*, **125**, 229–235 (2003).
24. G. Ferretti, C. Maffezzoni, and R. Scattolini, On the identifiability of the time delay with least-squares methods, *Automatica*, **32**, 449–453 (1996).
25. Y. Orlov, L. Belkoura, J. P. Richard, and M. Dambrine, On identifiability of linear time-delay systems, *IEEE Transactions on Automatic Control*, **47**, 1319–1324 (2002).
26. Z. Sun and X. Yang, Parameters identification and synchronization of chaotic delayed systems containing uncertainties and time-varying delay, *Mathematical Problems in Engineering*, 105309 (2010).
27. Y. Tang and X. Guan, Parameter estimation for time-delay chaotic systems by particle swarm optimization, *Chaos, Solitons and Fractals*, **40**, 1391–1398 (2009).
28. J. Zhang, X. Xia, and C. H. Moog, Parameter identifiability of nonlinear systems with time-delay, *IEEE Transactions on Automatic Control*, **51**, 371–375 (2006).
29. B. Mann and K. Young, An empirical approach for delayed oscillator stability and parametric identification, *Proceedings of the Royal Society A*, **462**, 2145–2160 (2006).
30. V. Deshmukh, Parametric estimation for delayed nonlinear time-varying dynamical systems, *Journal of Computational Nonlinear Dynamics*, **6**, 041003-1 (2011).
31. D. Eller, G. Aggarwal, and H. Banks, Optimal control of linear time-delay systems, *IEEE Transactions on Automatic Control*, **AC-14**, 678–687 (1969).
32. A. Manitius and A. Olbrot, Finite spectrum assignment problem for systems with delays, *IEEE Transactions on Automatic Control*, **24**, 541–553 (1979).
33. I.-R. Horng and J. -H. Chou, Analysis, parameter estimation and optimal control of time-delay systems via Chebyshev series, *International Journal of Control*, **41**, 1221–1234 (1985).
34. K. Engelborghs, M. Dambrine, and D. Roose, Limitations of a class of stabilization methods for delay systems, *IEEE Transactions on Automatic Control*, **46**, 336–339 (2001).

35. S. Mondie and W. Michiels, Finite spectrum assignment of unstable time-delay systems with a safe implementation, *IEEE Transactions on Automatic Control*, **48**, 2207–2212 (2003).
36. A. Ailon, R. Segev, and S. Arogeti, A simple velocity-free controller for attitude regulation of a spacecraft with delayed feedback, *IEEE Transactions on Automatic Control*, **49**, 125–130 (2004).
37. J. -Q. Sun and B. Song, Control studies of time-delayed dynamical systems with the method of continuous time approximation, *Communications in Nonlinear Systems and Numerical Simulation*, **14**(11), 3933–3944 (2009).
38. W. Michiels, T. Vyhlidal, and P. Zitek, Control design for time-delay systems based on quasi-direct pole placement, *Journal of Process Control*, **20**, 337–343 (2010).
39. A. Chunodkar and M. Akella, Attitude stabilization with unknown bounded delay in feedback control implementation, *Journal of Guidance, Control, and Dynamics*, **34**, 533–542 (2011).
40. M. Nazari, E. Samiei, E. Butcher, and H. Schaub, Attitude stabilization using nonlinear delayed actuator control with an inverse dynamics approach, 22*nd AIAA/AAS Space Flight Mechanics Meeting, Charleston, SC, USA* (Jan. 29–Feb. 2, 2012).
41. E. Samiei, M. Nazari, E. Butcher, and H. Schaub, Delayed feedback attitude control using neural networks and Lyapunov-Krasovskii functionals, 22*nd AIAA/AAS Space Flight Mechanics Meeting, Charleston, SC, USA* (Jan. 29–Feb. 2, 2012).
42. T. Insperger, Act and wait concept for time-continuous control systems with feedback delay, *IEEE Transactions on Control Systems*, **14**, 974–977 (2006).
43. T. Insperger and G. Stepan, Act-and-wait concept for discrete-time systems with feedback delay, *IET Control Theory A*, **1**, 553–557 (2007).
44. G. Stepan and T. Insperger, Stability of time-periodic and delayed systems — A route to act-and-wait control, *Annual Reviews in Control*, **30**, 159–168 (2006).
45. V. Deshmukh, H. Ma, and E. Butcher, Optimal control of parametrically excited linear delay differential systems via Chebyshev polynomials, *Optimal Control Applications and Methods*, **27**, 123–136 (2006).
46. H. Ma, E. Butcher, and E. Bueler, Chebyshev expansion of linear and piecewise linear dynamic systems with time delay and periodic coefficients under control excitations, *Journal of Dynamic Systems, Measurement, and Control*, **125**, 236–243 (2003).
47. H. Ma, V. Deshmukh, E. Butcher, and V. Averina, Delayed state feedback and chaos control for time-periodic systems via a symbolic approach, *Communications in Nonlinear Science and Numerical Simulation*, **10**, 479–497 (2005).
48. J. Zhang and J.-Q. Sun, Robustness analysis of optimally designed feedback control of linear periodic systems with time-delay, *Proceedings of the* 6*th International Conference on Multibody Systems, Nonlinear Dynamics, and Control*, ASME DETC 2007, Las Vegas, NV. (Sept. 4–7, 2007).
49. O. Elbeyli and J.-Q. Sun, On the semi-discretization method for feedback control design of linear systems with time delay, *Journal of Sound and Vibration*, **273**, 429–440 (2004).
50. J. Sheng and J.-Q. Sun, Feedback controls and optimal gain design of delayed periodic linear systems, *Journal of Vibration and Control*, **11**(2), 277–294 (2005).
51. J. Sheng, O. Elbeyli, and J.-Q. Sun, Stability and optimal feedback controls for time-delayed linear periodic systems, *AIAA Journal*, **42**(5), 908–911 (2004).
52. E. Butcher and O. Bobrenkov, On the Chebyshev spectral continuous time approximation for constant and periodic delay differential equations, *Communications in Nonlinear Science and Numerical Simulation*, **16**, 1541–1554 (2011).
53. O. Bobrenkov, E. Butcher, and B. Mann, On application of the Liapunov-Floquet

transformation to differential equations with time delay and periodic coefficients, *Journal of Vibration and Control* (2012). doi:10.1177/1077546311433914.
54. O. Diekmann, S. van Gils, S. Verduyn Lunel, and H.-O. Walther, *Delay Equations*: *Functional, Complex, and Nonlinear Analysis* (Springer-Verlag, New York, 1995).
55. A. Halanay, *Differential Equations*: *Stability, Oscillations, Time Lags* (Academic Press, New York, 1966).
56. J. Hale and S. Verduyn Lunel, *Introduction to Functional Differential Equations* (Springer-Verlag, New York, 1993).
57. J.-Q. Sun, A method of continuous time approximation of delayed dynamical systems, *Communications in Nonlinear Science and Numerical Simulation*, **14**(4), 998–1007 (2009).
58. D. Breda, S. Maset, and R. Vermiglio, Pseudospectral differencing methods for characteristic roots of delay differential equations, *SIAM Journal of Scientific Computing*, **27**(2), 482–495 (2005).
59. D. Breda, S. Maset, and R. Vermiglio, Computing the characteristic roots for delay differential equations, *IMA Journal of Numerical Analysis*, **24**, 1–19 (2004).
60. D. Breda, Solution operator approximations for characteristic roots of delay differential equations, *Applied Numerical Mathematics*, **56**, 305–317 (2006).
61. L. Trefethen, *Spectral Methods in MATLAB* (SIAM Press, Philadelphia, 2000).
62. P. Wahi and A. Chatterjee, Galerkin projections for delay differential equations, *Journal of Dynamic Systems, Measurement, and Control*, **127**, 80–87 (2005).
63. E. Bueler, Error bounds for approximate eigenvalues of periodic-coefficient linear delay differential equations, *SIAM Journal of Numerical Analysis*, **45**(6), 2510–2536 (2007).
64. L. Fox and I. B. Parker, *Chebyshev Polynomials in Numerical Analysis* (Oxford University Press, London, 1968).
65. C. Clenshaw, The numerical solution of linear differential equations in chebyshev series, *Proceedings of Cambridge Philosophical Society*, **53**, 134–149 (1957).
66. T. Insperger and G. Stépán, Stability chart for the delayed Mathieu equation, *Proceedings of Royal Society of London A*: *Mathematical, Physical, and Engineering Sciences*, **458**, 1989–1998 (2002).
67. C. Hsu and S. Bhatt, Stability charts for second-order dynamical systems with time lag, *Journal of Applied Mechanics* (*ASME*), **33E**(1), 119–124 (1966).
68. F. Van der Pol and M. J. O. Strutt, On the stability of the solutions of Mathieu's equation, *Philosophical Magazine and Journal of Science*, **5**, 18–38 (1928).
69. S. Sinha, R. Pandiyan, and J. Bibb, Liapunov-Floquet transformation: computation and applications to periodic systems, *Journal of Vibration and Acoustics*, **118**, 209–219 (1996).
70. S. Sinha, S. Redkar, and E. Butcher, Order reduction of nonlinear systems with time-periodic coefficients using invariant manifolds, *Journal of Sound and Vibration*, **284**, 985–1002 (2005).
71. S. Sinha, S. Redkar, V. Deshmukh, and E. Butcher, Order reduction of parametrically excited nonlinear systems: techniques and applications, *Nonlinear Dynamics*, **41**, 237–273 (2005).
72. A. Dávid and S. Sinha, Bifurcation control of nonlinear systems with time-periodic coefficients, *Journal of Dynamic Systems, Measurement, and Control*, **125**, 541–548 (2003).
73. S. Sinha and A. David, Control of chaos in nonlinear systems with time-periodic Coefficients, *Philosophical Transactions of the Royal Society A*, **364**, 2417–2432 (2006).
74. E. B. S. C. Sinha and A. Dávid, Construction of dynamically equivalent time-

invariant forms for time-periodic systems, *Nonlinear Dynamics*, **16**, 203–221 (1998).
75. E. Butcher and S. Sinha, Canonical perturbation of a fast time-periodic Hamiltonian via Liapunov-Floquet transformation, *Journal of Applied Mechanics*, **65**, 209–217 (1998).
76. T. Kalmár-Nagy, G. Stépán, and F. Moon, Subcritical Hopf bifurcation in the delay equation model for machine tool vibrations, *Nonlinear Dynamics*, **26**, 121–142 (2001).
77. S. Zhao and T. Kalmár-Nagy, *Center Manifold Analysis of the Delayed Liénard Equation*, 203–220 (Delay Differential Equations: Recent Advances and New Directions, B. Balachandran, T. Kalmár-Nagy, and D. Gilsinn (Eds.), Springer, 2009).
78. D. Gilsinn, Estimating critical Hopf bifurcation parameters for a second-order delay differential equation with application to machine tool chatter, *Nonlinear Dynamics*, **30**, 103–154 (2002).
79. V. Deshmukh and E. Butcher, Dimensional reduction of nonlinear delay differential equations with periodic coefficients using Chebyshev spectral collocation, *Nonlinear Dynamics*, **52**, 137–149 (2008).
80. A. Nayfeh, Order reduction of retarded nonlinear systems — the method of multiple scales versus center-manifold reduction, *Nonlinear Dynamics*, **51**, 483–500 (2008).
81. E. Butcher and S. Sinha, A hybrid formulation for the analysis of time-periodic linear systems via Chebyshev polynomials, *Journal of Sound and Vibration*, **195**, 518–527 (1996).
82. L. Moreau and D. Aeyels, Periodic output feedback stabilization of single-input single-output continuous-time systems with odd relative degree, *Systems and Control Letters*, **51**, 395–406 (2004).
83. J. Allwright, A. Astolfi, and H. Wong, A note on asymptotic stabilization of linear systems by periodic, piecewise constant output feedback, *Automatica*, **41**, 339–344 (2005).
84. A. David and S. Sinha, Some ideas on the local control of nonlinear systems with time-periodic coefficients, *Proceedings of the ASME Design Engineering Technical Conferences, Las Vegas, NV*, 1–10 (Sept. 12–15, 1999).
85. S. Sinha, E. Gowrdon, and Y. Zhang, Control of time-periodic systems via symbolic computation with application to chaos control, *Communications in Nonlinear Science and Numerical Simulation*, **10**, 835–854 (2005).
86. S. Sinha, J. Henrichs, and B. Ravindra, A general approach in the design of active controllers for nonlinear systems exhibiting chaos, *International Journal of Bifurcation and Chaos*, **10**, 165–178 (2000).
87. S. Sinha and P. Joseph, Control of general dynamic systems with periodically varying parameters via Liapunov-Floquet transformation, *Journal of Dynamic Systems, Measurement, and Control*, **116**, 650–658 (1994).
88. V. Deshmukh and S. Sinha, Control of dynamic systems with time-periodic coefficients via the Lyapunov-Floquet transformation and backstepping technique, *Journal of Vibration and Control*, **10**, 1517–1533 (2004).
89. R. Pandiyan and S. Sinha, Time-varying controller synthesis for nonlinear systems subjected to periodic parametric loadings, *Journal of Vibration and Control*, **7**, 73–90 (2001).
90. V. Deshmukh, S. Sinha, and P. Joseph, Order reduction and control of parametrically excited dynamical systems, *Journal of Vibration and Control*, **6**, 1017–1028 (2000).
91. S. Sinha and R. Pandiyan, Analysis of quazilinear systems with periodic coefficients via Liapunov-Floquet transformation, *International Journal of Non-Linear Mechanics*, **29**(5), 687–702 (1994).

92. E. A. Butcher, H. Ma, E. Bueler, V. Averina, and Z. Szabó, Stability of linear time-periodic delay-differential equations via Chebyshev polynomials, *International Journal Numerical Methods in Engineering*, **59**, 895–922 (2004).
93. A. Gabale and S. Sinha, Model reduction of nonlinear systems with external periodic excitations via construction of invariant manifolds, *Journal of Sound and Vibration*, **330**(11), 2596–2607 (2011).
94. J. Speyer and W. Chung, *Stochastic Processes, Estimation, and Control* (*Advances in Design and Control*) (SIAM, Philadelphia, PA, 2008).
95. A. Jazwinski, *Stochastic Processes and Filtering Theory* (Academic, New York, 1970).
96. S. Sinha and Y. Zhang, Observer design for nonlinear systems with time-periodic coefficients via normal form theory, *Journal of Computational and Nonlinear Dynamics*, **4**(3), 031001 (2009).
97. L. Shampine and S. Thompson, Solving delay differential equations in MATLAB, *Applied Numerical Mathematics*, **37**(4), 441–458 (2001).
98. G. Welch, *SCAAT*: *Incremental Tracking with Incomplete Information* (PhD dissertation, University of North California at Chapel Hill, 1996).
99. H. Schaub and J. Junkins, *Analytical Mechanics of Space Systems* (AIAA, Reston, VA, USA, 2009).
100. R. Paielli and R. Bach, Attitude control with realization of linear error dynamics, *Journal of Guidance, Control, and Dynamics*, **16**, 182–189 (1993).